Review: Measurement of Partial Electrical Conductivities and Transport Numbers of Mixed Ionic-electronic Conducting Oxides

Yue Huang [a†], Ruiming Qiu [a†], Wenchao Lian [a], Libin Lei [a*], Tong Liu [b], Jihao Zhang [c], Yao Wang [b], Jianping Liu [a], Jin Huang [d], Fanglin Chen [e]

[a] Smart Energy Research Center, School of Materials and Energy, Guangdong University of Technology, Guangzhou 510006, PR China.

[b] School of Power and Mechanical Engineering, Wuhan University, Wuhan, Hubei 430072, PR China.

[c] School of Electrical and Power Engineering, China University of Mining and Technology, Xuzhou, 221116, PR China.

[d] Faculty of electric engineering, Guangdong Polytechnic of Water Resources and Electric Engineering, Guangzhou 510925, PR China.

[e] Department of Mechanical Engineering, University of South Carolina, Columbia, SC 29208, USA.

† These authors contributed equally.

*Corresponding author: E-mail: libinlei23@gdut.edu.cn

Abstract: Mixed ionic-electronic conducting (MIEC) oxides play crucial roles in energy and environmental applications such as fuel cells, electrolysis cells, batteries, gas separation membranes, and membrane reactors for chemical synthesis. The application of MIEC oxides is primarily determined by their electrical conduction properties. Correctly measuring the electrical conduction

properties of MIEC oxides, including the partial conductivity and corresponding transport numbers, is fundamental for the development of MIEC oxides. In this review, the theoretical principles and experimental techniques of the five most widely used methods for determining electrical conduction properties of MIEC oxides, namely the total conductivity measurement (section 2), the electromotive force method (section 3), the Faradaic efficiency method (section 4), the Hebb-Wagner method (section 5), and the gas permeation method (section 6), are summarized. The modifications of these methods by considering the electrode polarization and operation conditions (under a certain voltage and current) are discussed. Application of these methods to assess the conduction properties of triple ionic-electronic conducting (TIEC) oxides is highlighted. Most importantly, the reliability and applicability of these methods are elaborated and compared (Section 7). This review is expected to provide an updated and informative summary concerning determination of the partial conductivities and transport numbers of MIEC oxides.

Keywords: mixed ionic-electronic conducting oxides; triple ionic-electronic conducting oxides, partial electrical conductivity; transport numbers; electrical conductivity measurement

Nomenclature

Nomenclature

Abbreviation

EIS	AC electrochemical impedance spectroscopy
EMF	Electromotive force
FE	Faradaic efficiency
GC	Gas chromatography
GP	Gas permeation
H-W	Hebb-Wagner
MIEC	Mixed ionic-electronic conducting
OCV	Open circuit voltage
SOEC	Solid oxide electrolysis cell
SOFC	Solid oxide fuel cell
TIEC	Triple ionic-electronic conducting

Greek letters

$\boldsymbol{\alpha}$	Four times of characteristic exponent ($\alpha = 4\|N\|$)
$\boldsymbol{\mu}$	Chemical potential (J/mol)
$\boldsymbol{\tilde{\mu}}$	Electrochemical potential (J/mol)
$\boldsymbol{\eta}$	Electrode overpotential (V)
$\boldsymbol{\sigma}$	Conductivity (S/m)
$\boldsymbol{\sigma^{\theta}}$	The conductivity at $P_{O_2} = 1\ atm$ (S/m)
$\boldsymbol{\sigma_{tot}}$	Total conductivity (S/m)

Subscripts or superscripts

$\boldsymbol{e}$	Electronic charge carrier
$\boldsymbol{e'}$	n-type electronic defect
$\boldsymbol{h^{\cdot}}$	Electron-hole (p-type electronic defect)
$\boldsymbol{H}$	Proton
$\boldsymbol{i}$	Ionic charge carrier
$\boldsymbol{j}$	Charge carrier
$\boldsymbol{O}$	Oxygen ion
$\boldsymbol{\ddot{O}}$	Oxygen vacancy
X	Active species

English letters

$\boldsymbol{D}$	Diffusion coefficient (m^2/s)
$\boldsymbol{D_x^{\theta}}$	Pre-exponential factor of diffusivity (m^2/s)
$\boldsymbol{E_{th}}$	Theoretical equilibrium voltage (V)
$\boldsymbol{F}$	Faraday constant (96485 C/mol)
$\boldsymbol{I}$	Current density (A/m^2)
$\boldsymbol{I_{ext}}$	The external current density (A/m^2)
J	Species flux ($mol\ m^{-2}\ s^{-1}$)
$\boldsymbol{K}$	Equilibrium constant
$\boldsymbol{k}$	Surface exchange coefficient
$\boldsymbol{k_B}$	Boltzmann constant (1.381×10^{-23} J/K)
$\boldsymbol{L}$	Thickness (μm)
$\boldsymbol{L_c}$	The characteristic thickness (μm)
$\boldsymbol{P}$	Operating pressure (atm)
$\boldsymbol{P_{O_2}^t}$	The actual oxygen partial pressure on the surfaces (atm)
$\boldsymbol{q}$	Elementary charge (1.602×10^{-19} C)
$\boldsymbol{R}$	Gas constant (8.3145 J/mol·K)
$\boldsymbol{R_{aux}}$	External variable resistance ($\Omega \cdot m^2$)
$\boldsymbol{R_{p,r}}$	Real electrode polarization resistance ($\Omega \cdot m^2$)
$\boldsymbol{R_s}$	Ohmic resistance of samples ($\Omega \cdot m^2$)
$\boldsymbol{R_T}$	Total resistances of cells ($\Omega \cdot m^2$)
$\boldsymbol{t}$	Transport numbers
$\boldsymbol{t_i^{app}}$	Apparent ionic transport number
$\boldsymbol{T}$	Temperature (K)
$\boldsymbol{V_{ocv}}$	Open circuit valtage (V)
$\boldsymbol{V_{out}}$	Output voltage (V)
$\boldsymbol{[X]_L}$	Formula-unit molar concentration
$\boldsymbol{z}$	Charge valence

1. Introduction

Mixed ionic-electronic conducting (MIEC) oxides simultaneously possess both ionic and electronic conduction. In the past few decades, MIEC oxides have drawn much attention due to their wide range of applications to address energy and environmental concerns [1]. Figure 1 (a) displays the number of published SCI papers regarding MIEC materials, mostly MIEC oxides. It is clear that since 2000, the number of papers has grown steadily, suggesting increasing research interest. To date, MIEC oxides have been widely applied in the fields of solid oxide fuel cells (SOFCs), solid oxide electrolysis cells (SOECs), batteries, gas separation membranes, membrane reactors, gas pumps, gas sensors, and so on [2-6]. Figure 1 (b) presents the co-occurrence network of keywords in SCI papers about MIEC materials, which is generated on VOSviewer software. The size and color of the node represent the usage frequency of the keywords and the research cluster respectively. The thickness of the connection line shows the link strength between different keywords. The keywords of MIEC and SOFC co-occur the most, suggesting the wide application of MIEC oxides in SOFCs. The keyword of MIEC also occurs in conjunction with oxygen permeation/separation or membrane. In addition, the keyword of electrochemical impedance spectroscopy (EIS) is found. This is because EIS, as a powerful electrochemical analysis tool, is frequently used in the characterization of MIEC oxides, which will be discussed in the following sections.

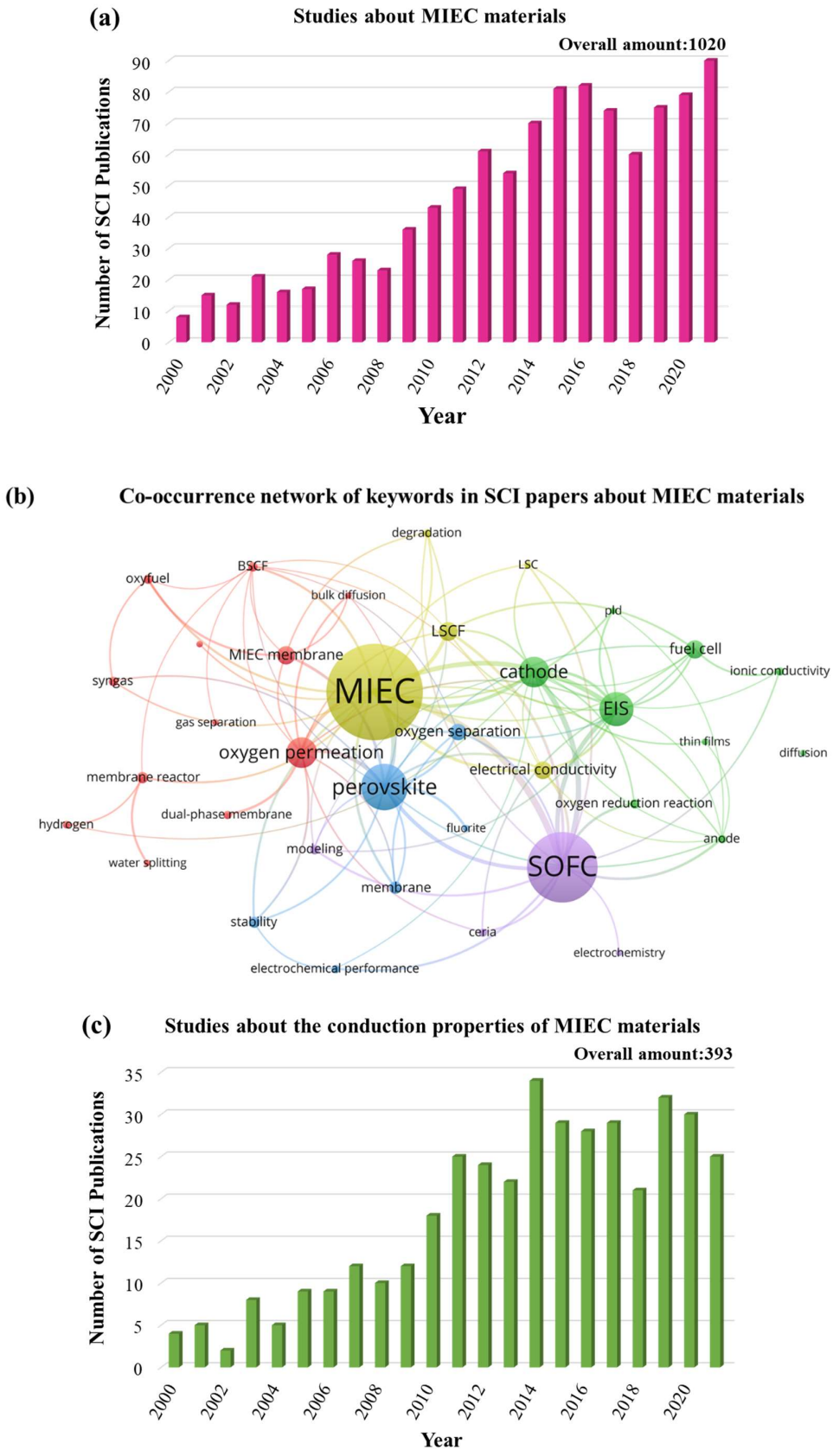
(a)
Studies about MIEC materials
Overall amount:1020
Number of SCI Publications
Year
(b)
Co-occurrence network of keywords in SCI papers about MIEC materials
degradation
BSCF
LSC
oxyfuel
bulk diffusion
pld
LSCF
fuel cell
MIEC membrane
cathode
ionic conductivity
syngas
MIEC
EIS
gas separation
oxygen separation
thin films
diffusion
oxygen permeation
electrical conductivity
membrane reactor
perovskite
oxygen reduction reaction
dual-phase membrane
hydrogen
fluorite
anode
modeling
water splitting
SOFC
membrane
stability
ceria
electrochemistry
electrochemical performance
(c)
Studies about the conduction properties of MIEC materials
Overall amount:393
Number of SCI Publications
Year

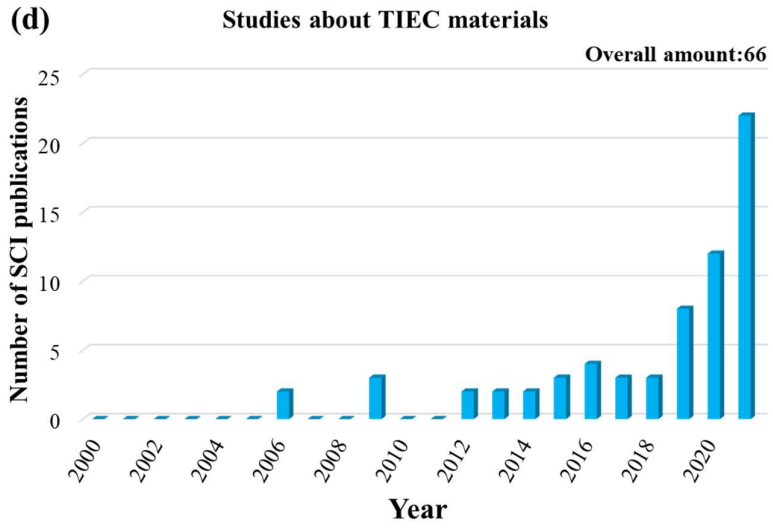

Figure 1 Scientometric analysis of SCI papers from 2000 to 2021 (a) annual SCI papers about MIEC materials; (b) co-occurrence network of keywords in SCI papers; (c) annual SCI papers about conduction properties of MIEC materials; (d) annual SCI papers about TIEC materials.

The electrical conduction properties of mixed ionic-electronic conducting oxides include the ionic conductivity (oxygen ion or proton), electronic conductivity (electron or electron hole), and transport numbers (t_j). The transport number is defined as the ratio of the partial electrical conductivity to the total electrical conductivity (σ_{tot}) [7]:

$$t_j = \frac{\sigma_j}{\sigma_{tot}} = \frac{\sigma_j}{\sum_j^n \sigma_j} == \frac{1/R_j}{\sum_j^n 1/R_j} \quad (1.)$$

$$\sum_j^n t_j = 1 \quad (2.)$$

where j, σ_j and R_j represent the type of charge carrier, conductivity and resistance respectively. When mixed ionic-electronic conducting oxides simultaneously accommodate two types of ionic conductivity (σ_i) and electronic conductivity (σ_e), they are also called triple ionic-electronic conducting (TIEC) oxides [8]. The TIEC oxides mentioned in this paper are referred in particular to those exhibiting oxygen-ionic

conductivity (σ_O), protonic conductivity (σ_H), and electronic conductivity (σ_e). The oxygen-ionic conductivity, protonic conductivity, and electronic conductivity are due to the formation of oxygen vacancies ($V_O^{\bullet\bullet}$), proton defects ($OH^{\bullet}$) and electron defects (e' or $h^{\cdot}$) respectively.

Depending on the types of crystal structure, MIEC oxides can be mainly classified as perovskite structure and fluorite structure. As shown in Figure 1 (b), the keyword of perovskite has a strong connection with MIEC, suggesting that a large number of MIEC oxides possess perovskite structure. Perovskite structure can be subdivided into three families, namely the simple perovskite structure (ABO_3), the layered perovskite structure ($AA'B_2O_6$) and the Ruddlesden-Popper structure ($A_{n+1}B_nO_{3n+1}$). All these perovskite-related structures possess an oxygen 6-fold coordinated transition metal scaffold (BO_6) [9]. The compounds of lanthanum strontium cobalt ferrite (LSCF) family, which have been widely studied and applied to SOFCs, SOECs and gas separation membranes, are typical ABO_3-type MIEC oxides [10, 11]. Layered $Ln_2NiO_{4+\delta}$ nickelates (Ln=La, Nd or Pr), as widely studied Ruddlesden-Popper (RP) phase MIEC materials, have some unique advantages, such as high chemical stability, high surface exchange coefficients, and improved oxygen-ion transport. They are also considered to show triple conducting behavior, when the proton uptake by the oxygen vacancies is thermodynamically favored [12]. The fluorite structure consists of anions in simple cubic packing with half the interstices filled by cations. It can be represented by AO_2, where A is large four valent cations such as Zr^{4+} and Ce^{4+}. A typical fluorite-structure MIEC oxide is ceria, which can also be found in the co-occurrence network

of keywords in the purple research cluster (Figure 1 (b)). The acceptor-doped ceria, such as Gd or Sm doped CeO_2 (GDC or SDC), show high oxygen-ion conductivity in an oxidizing atmosphere and mixed ionic-electronic conduction in a reducing atmosphere, due to the partial reduction of Ce^{4+} to Ce^{3+} [13].

The application of mixed ionic-electronic conducting oxides is primarily determined by their electrical conduction properties. When used as the electrolyte materials of solid oxide fuel cells, solid oxide electrolysis cells and gas pumps, MIEC are required to possess reasonable ionic conductivity and negligible electronic conductivity. In other words, the ionic transport number should be as large as possible, especially in the cases of solid oxide electrolysis cells and gas pumps since the decrease in ionic transport number leads to a significant decline in the Faradaic efficiency and energy efficiency [14-16]. By contrast, when MIEC oxides are applied as the electrode materials of SOFCs, SOECs and batteries, possessing both ionic and electronic conductivities is beneficial to enhancing their performance. Notably, to efficiently extend the active reaction sites, triple ionic-electronic conductors are desired as the electrode materials of proton conducting solid oxide fuel cells (H-SOFCs) and proton conducting solid oxide electrolysis cells (H-SOECs) [8, 17-21]. As for the gas separation membranes, MIEC oxides should exhibit both ionic and electronic conductivities as large as possible for achieving high gas permeability.

Correctly measuring the partial conductivity and transport numbers of mixed ionic-electronic conducting oxides is fundamental and essential for the development of MIEC oxides. In recent years, many efforts have been devoted to designing and

developing new MIEC oxides for different applications [8, 12, 22]. The electrical conduction properties of MIEC oxides are dictated by their chemical composition, crystal structure, microstructure, gas atmosphere and so on [23]. Precisely determining the electrical conduction properties of MIEC oxides is the premise of understanding the relationships between the electrical conduction properties and the above influencing factors, which are important guidelines for designing and applying MIEC oxides. Since ionic and electronic conductivity or oxygen-ionic and protonic conductivity have to be separated, the measurement of partial conductivities and transport numbers of MIEC oxides is more complicated, compared with the cases of pure ionic or electronic conductors.

To measure the partial conductivities and transport numbers of mixed ionic-electronic conducting oxides, a number of methods have been developed. Among these methods, total conductivity measurement, electromotive force (EMF) method, Faradaic efficiency (FE) method, Hebb-Wagner (H-W) method, and gas permeation (GP) method are the most widely used. The basic principles of these five methods are different and the determination of conduction properties by these five methods is based on different types of experimental data, such as resistance, voltage, current, and gas composition. However, the reviews on these five approaches are relatively scarce. In 1996, the use of the Hebb-Wagner method for determining partial conductivities of MIEC oxides and the limitation of this method were reviewed by Riess [24]. In 2004, Naumovich *et al.* [25] briefly summarized the basic principles of the electromotive force, gas permeation, and Faradaic efficiency methods for determining conduction

properties of mixed oxygen-ionic and electronic conductors. In 2014, Prakangas *et al.* [26] reviewed the methods for measuring the ionic conductivity of doped ceria/carbonate composite materials. These methods can be classified as impedance measurement, constant current measurement, and product analysis measurement. Afterward, to the best of our knowledge, no review has been conducted on the measurement of electrical conduction properties of MIEC oxides. In the past decade, significant progress has been made in improving the reliability and applicability of these five methods [27]. From Figure 1 (c), it can be seen that the number of published SCI articles concerning the electrical conduction characteristics of MIEC oxides gradually increases, indicating the significance of the determination of electrical conduction properties. Among these publications, some are concerning the improvement of measurement methods. Moreover, TIEC materials have garnered growing research attention, which is attributed to their unique benefits as electrode materials [12, 28, 29]. Some well-known oxygen-ionic conducting electrolyte materials, such as Sr and Mg co-doped $LaGaO_3$ (LSGM), have been experimentally demonstrated to show proton conduction in a hydrogen-containing atmosphere [30, 31]. Recently, $BaCe_{1-x}Zr_xO_3$-based oxides, which are the most used protonic conducting electrolyte materials, have been experimentally [32] and theoretically [33, 34] demonstrated to possess protonic, oxygen ionic, and electronic conductivities simultaneously at high temperatures (above 873 K) in a wet and oxidizing atmosphere. Figure 1 (d) presents the number of SCI papers published for TIEC oxides from 2000 to 2021. Prior to 2012, the researches on TIEC oxides are scarce. After 2012, TIEC oxides began to receive

more and more attention. Significant growth in the number of papers is observed in the past three years (2019-2021). For TIEC oxides, identification of different ionic charge carriers and their corresponding transport numbers is complicated and difficult. Until now, there hasn't been a systematical summary for measuring the electrical conduction properties of TIEC oxides. In addition, it is noteworthy that due to the misusage or inappropriate simplification of some of these methods, the characterization of electrical conduction properties of MIEC oxides could lead to inconsistent data and controversial conclusions [35]. Therefore, researchers working on MIEC oxides would benefit greatly from an updated, comprehensive, and in-depth review regarding the methods in determining the electrical conduction properties of MIEC oxides.

This review aims at summarizing the theoretical and experimental progress of the five most widely used methods for determining the electrical conduction properties of mixed ionic-electronic conducting oxides, namely the total conductivity measurement (section 2), the EMF method (section 3), the FE method (section 4), the H-W method (section 5), and the GP method (section 6), as displayed in Figure 2. Modifications of these measurement methods by considering electrode polarization, operation conditions (under voltages and currents), and triple charge carriers are discussed. In addition, the most recent research advancements of these methods are particularly highlighted. Most importantly, the reliability and applicability of these five methods are elaborated and compared (section 7). This review is expected to provide an updated, informative, and in-depth summary concerning determination of the partial conductivities and transport numbers of MIEC oxides.

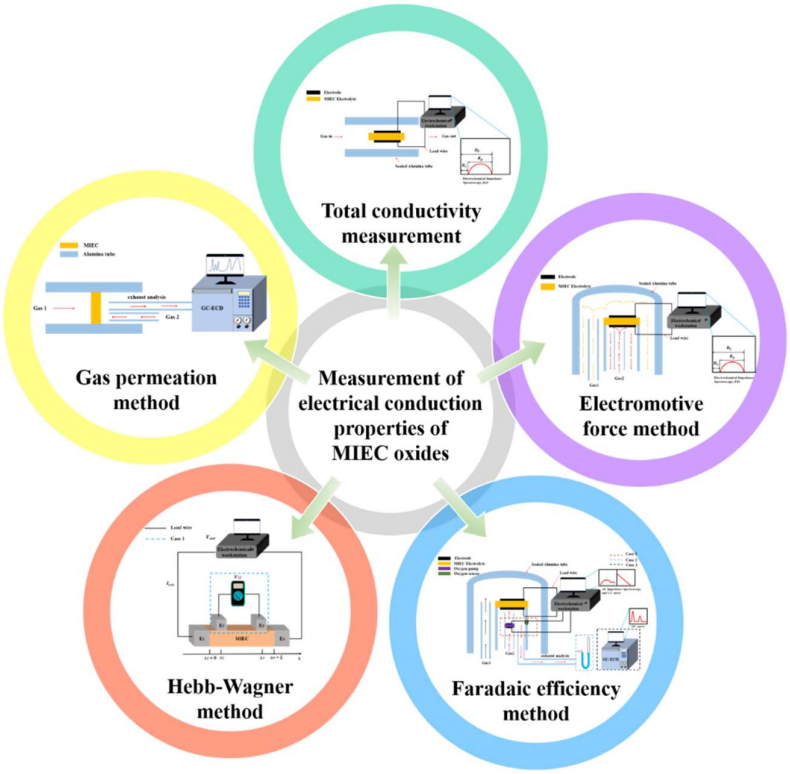

Figure 2 Five most widely used methods for determining electrical meconduction properties of MIEC oxides

2. Total conductivity measurement (Patterson diagrams)

2.1 The basic principles of total conductivity measurement

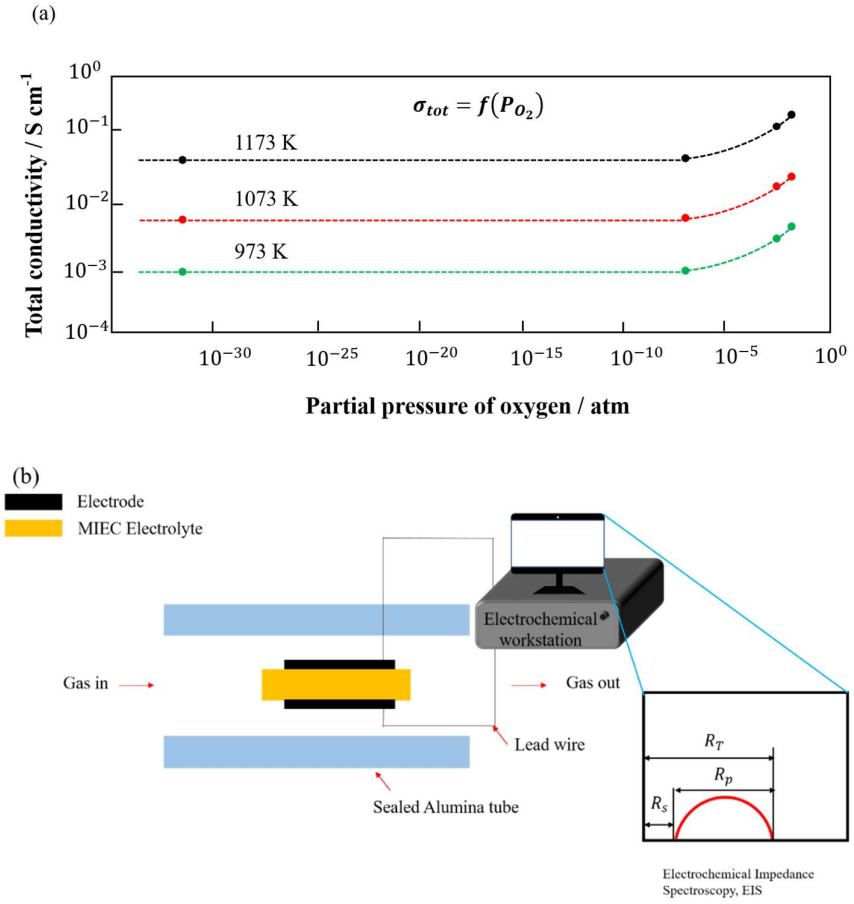

Figure 3 (a) Schematic of Patterson diagram; (b) schematic of test setup for measuring total conductivity by electrochemical impedance spectroscopy.

This method was initially proposed by J. W. Patterson [36] in 1971. The basic principle of this method is based on the relationship between the total conductivity of the sample and oxygen partial pressure (Patterson diagrams). Figure 3 (a) is a schematic illustration of Patterson diagram, drawn by us, and it schematically shows the change of total conductivity of an MIEC sample at various oxygen partial pressures and temperatures. It is well known that the total conductivity (σ_{tot}) of a mixed ionic-

electronic conducting oxide is the sum of the ionic conductivity (σ_i) and electronic conductivity (σ_e). Generally speaking, if the oxygen partial pressure (P_{O_2}) is not in a large range, the ionic conductivity can be assumed to be constant. By contrast, both n-type and p-type electronic conductivities are significantly governed by oxygen partial pressure. Taking mixed oxygen-ionic and electronic conductors as an example, such as acceptor-doped ceria, the predominant electronic conductivity is n-type ($\sigma_{e'}$), which is proportional to $P_{O_2}^{-\frac{1}{4}}$. Thus, the total conductivity can be expressed as [37]:

$$\sigma_{tot} = \sigma_O + \sigma_{e'}^{\theta} P_{O_2}^{-\frac{1}{4}} \tag{3.}$$

where $\sigma_{e'}^{\theta}$ is the electronic conductivity at $P_{O_2} = 1\ atm$. σ_O and $\sigma_{e'}^{\theta}$ can be easily obtained by fitting the data of the total conductivity as a function of oxygen partial pressure. σ_O is a function of temperature and obeys an Arrhenius relation with the activation energy of oxygen-ion migration (ΔH_O). While $\sigma_{e'}^{\theta}$ is also a function of temperature and obeys an Arrhenius relation with an apparent, or combined activation energy of $\Delta H_{e',o}$, which is the sum of real activation energy of electron migration ($\Delta H_{e'}$) and one half of the reduction enthalpy (ΔH_r) of Ce^{4+} [37].

Similarly, in the case of mixed protonic and electronic conducting oxides, the total conductivity is the sum of protonic conductivity (σ_H) and electron-hole conductivity ($\sigma_{h\cdot} \propto P_{O_2}^{\frac{1}{4}}$) [32, 38]:

$$\sigma_{tot} = \sigma_H + \sigma_{h\cdot}^{\theta} P_{O_2}^{\frac{1}{4}} \tag{4.}$$

where $\sigma_{h\cdot}^{\theta}$ is the electron-hole conductivity at $P_{O_2} = 1\ atm$. The electrical conduction properties can also be readily determined by fitting the experimental data. Notably, σ_H

is a function of both temperature and humidity. While the mathematical relation between σ_h^{θ}. and temperature is relatively complex, which can be found in the literature [39].

The schematic experimental setup of the total conductivity measurement method is shown in Figure 3 (b). The gas with strictly known oxygen partial pressure is fed to the chamber. The pellet-like or rod-like sample with two electrodes (Pt or Ag) is placed in a chamber at a specific temperature. AC electrochemical impedance spectroscopy (EIS) can be used to measure the total conductivity (ohmic resistance) of the sample [40]. For EIS, 2 or 4-probe method can be applied. The resistance of the lead wires and the contact resistance can be excluded by using the 4-probe method. When the effect of grain boundary resistance can be excluded, in the Nyquist plot of EIS the intercept of the real axis at high frequency corresponds to the ohmic resistance of the sample (R_S):

$$\lim_{\omega \to \infty} \{Z\} = R_s = \frac{L}{\sigma_{tot}} \quad (5.)$$

where L is the thickness of the mixed ionic-electronic conducting sample. Besides AC electrochemical impedance spectroscopy, DC van der Pauw method can also be used to measure the total conductivity. More information about van der Pauw method can be found in the literature [41]. The total conductivity of the sample is measured as a function of temperature and oxygen partial pressure. Various oxygen partial pressures are obtained usually in two approaches: specific gas mixtures and P_{O_2} -regulated electrochemical cells [42]. A relatively high range of oxygen partial pressure (10^{-3} -1 atm) can be obtained by precisely mixing oxygen or air with inert gases (N_2, Ar, He). For the low range of oxygen partial pressure (10^{-30}-10^{-10} atm), mixture gases of H_2+H_2O

or $CO+CO_2$ are used. The chemical stability of MIEC oxides in a CO or CO_2-containing atmosphere should be considered.

2.2 The modification of the total conductivity measurement method

In the above discussion, one important assumption (constant ionic conductivity over the entire range of oxygen partial pressure) is applied. However, because of the constraints of site conservation and local charge neutrality, the concentration of ionic charge carriers may change, leading to non-negligible variations of ionic conductivity. Thus, the way of calculating total and partial conductivities should be modified. Taking Gd-doped ceria as an example, the equilibrium between oxygen vacancy ($V_O^{\bullet\bullet}$) and polaron (Ce'_{Ce}) exists:

$$2Ce_{Ce}^{\times} + O_O^{\times} \leftrightarrow 2Ce'_{Ce} + V_O^{\bullet\bullet} + \frac{1}{2}O_2 \quad \text{(I)}$$

$$K = \frac{[Ce'_{Ce}]_L^2 \cdot [V_O^{\bullet\bullet}]_L \cdot (P_{O_2})^{1/2}}{[Ce_{Ce}^{\times}]_L^2 \cdot [O_O^{\times}]_L} \quad \text{(6.)}$$

where $[X]_L$ is the formula-unit molar concentration of X and K is the temperature-dependent equilibrium constant. Moreover, the site conservation and electroneutrality require:

$$[V_O^{\bullet\bullet}]_L + [O_O^{\times}]_L = 2 \quad \text{(7.)}$$

$$[Ce'_{Ce}]_L + [Gd'_{Ce}]_L + [Ce_{Ce}^{\times}]_L = 1 \quad \text{(8.)}$$

$$2[V_O^{\bullet\bullet}]_L = [Ce'_{Ce}]_L + [Gd'_{Ce}]_L \quad \text{(9.)}$$

According to the Nernst-Einstein relation, the partial conductivity can be calculated by:

$$\sigma_O = \frac{(2F)^2[V_O^{\bullet\bullet}]}{RT} D_O \quad (10.)$$

$$\sigma_{e'} = \frac{(F)^2[Ce'_{Ce}]}{RT} D_e \quad (11.)$$

$$D_x = D_x^{\theta} \exp\left(-\frac{E_x}{RT}\right) \quad (12.)$$

where F is the Faraday constant, R is the ideal gas constant , T is the temperature, D_x is the diffusivity, D_x^{θ} is pre-exponential factor of diffusivity and E_x is the activation energy of diffusivity. Combing eqs. (10) and (11), the total conductivity can be represented as:

$$\sigma_{tot} = \frac{(2F)^2[V_O^{\bullet\bullet}]}{RT} D_O + \frac{F^2[Ce'_{Ce}]}{RT} D_{e'} \quad (13.)$$

Through solving eq. (6-9,12-13) and fitting the experimental data of the total conductivity at various oxygen partial pressures and temperatures, the parameters of conduction properties can be obtained. Recently, considering site conservation and local charge neutrality, Sandrine *et al.* [40] and Zhu *et al.* [43] have conducted studies to determine the conduction properties of Gd doped ceria by fitting the total conductivity of the samples. Although fitting the total conductivity data with considering the site conservation and local charge neutrality is more accurate in theory, it could be difficult to unambiguously determine a complete set of conduction properties due to the existence of multi mathematical solutions. Hence, incorporating conductivity measurement at both steady state and transient state is feasible to eliminate the uncertainty [43]. The conductivity measurement at the transient state, also known

as electrical conductivity relaxation (ECR) method, requires an extra and complicated experimental setup, such as rapid gas switching system. In addition, the measurement of ohmic resistance of the sample needs to be completed in a short time. The ECR method is usually used to determine the bulk diffusion coefficient (D_{chem}) and the chemical surface exchange coefficient (k_{chem}) of MIEC oxides [44-47]. Moreover, thermogravimetric (TG) analysis [13, 48] or coulometric titration [49] can provide additional information on defect concentrations, which can help reduce the amount of the fitting parameters and mitigate the uncertainty in fitting the conductivity data.

2.3 The case of triple ionic-electronic conducting oxides

For triple ionic-electronic conducting oxides, oxygen-ionic, protonic, and electronic conductivities simultaneously contribute to the total conductivity. Thus the total conductivity is expressed as:

$$\sigma_{tot} = \sigma_O + \sigma_H + \sigma_e \quad (14.)$$

The conduction properties of triple ionic-electronic conducting oxides, such as $BaZr_{0.8}Y_{0.2}O_{3-\delta}$ (BZY) and $BaCe_{0.7}Zr_{0.1}Y_{0.1}Yb_{0.1}O_{3-\delta}$ (BZCYYb), have been investigated [33, 34]. Moreover, because protonic conductivity is generally positively related to the humidity of an atmosphere, the electrical conduction properties of triple ionic-electronic conducting oxides at various humidities can also be evaluated as experimental data for fitting [50, 51]. Since the situations of triple ionic-electronic conducting oxides are more complex than those with only two charge carriers and the mathematical uncertainty of fitting, the determination of conduction properties of triple ionic-electronic conducting oxides by total conductivity measurement warrants further

study. It is possible to improve the reliability of results obtained by the total conductivity measurement method, with the help of other methods listed above (measurement of transient conductivity, thermogravimetric analysis and coulometric titration).

3. Electromotive force (EMF) method

3.1 The basic principles of EMF method

EMF method is one of the most widely used approaches to estimate the electrical conduction properties of mixed ionic-electronic conducting oxides. The classical EMF method is based on the measurement of the open-circuit voltage (OCV, V_{ocv}) of a cell consisting of a mixed ionic-electronic conducting oxide as the electrolyte with two reversible electrodes subject to a chemical potential gradient. According to the Wagner theory, V_{ocv} is determined by [52]:

$$V_{ocv} = \frac{1}{zF}\int_{\mu_X'}^{\mu_X''} t_i d\mu_X \tag{15.}$$

where μ_X is the chemical potential of active species X and t_i is the ionic transport number. In the case of the mixed oxygen-ionic and electronic conducting oxide ($t_i = t_o$), eq. (15) can be rewritten as:

$$V_{ocv} = \frac{1}{4F}\int_{\mu_{O_2}'}^{\mu_{O_2}''} t_i d\mu_{O_2} = \frac{RT}{4F}\int_{P_{O_2}'}^{P_{O_2}''} t_i d\ln\left(P_{O_2}\right) \tag{16.}$$

Intergrating eq. (16):

$$t_i^{app} = \frac{V_{ocv}}{\frac{RT}{4F}\ln\frac{P_{O_2}''}{P_{O_2}'}} = \frac{V_{ocv}}{E_{th}} \tag{17.}$$

where E_{th} $(= \frac{RT}{4F}\ln\frac{P_{O_2}''}{P_{O_2}'})$ is the theoretical equilibrium voltage and t_i^{app} is the apparent ionic transport number. Because of the different oxygen partial pressures at the two

electrodes, ionic transport number isn't constant across the MIEC electrolyte layer and the calculated t_i^{app} from eq. (17) is the apparent ionic transport number subjected to a given gradient of oxygen pressure.

The principles of the EMF method can also be illustrated in terms of equivalent circuits, as shown in Figure 4 (a). The equivalent circuit of the classical EMF consists of E_{th}, ionic resistance (R_i), and electronic resistance (R_e) of the MIEC electrolyte. According to Kirchoff's law, the electrical potentials and resistances satisfy the following relation under open circuit condition ($V_{out} = V_{ocv}$):

$$\frac{E_{th}-V_{ocv}}{R_i} = \frac{V_{ocv}}{R_e} \qquad (18.)$$

It can also be deduced that t_i^{app} is equal to the ratio of V_{ocv} and E_{th}:

$$t_i^{app} = \frac{R_e}{R_i+R_e} = \frac{V_{ocv}}{E_{th}} \qquad (19.)$$

The ionic conductivity (σ_i) and electronic conductivity (σ_e) can be calculated by the following equations:

$$\sigma_i = \frac{L}{R_i} = \frac{LV_{ocv}}{E_{th}R_S} \qquad (20.)$$

$$\sigma_e = \frac{L}{R_e} = \frac{L}{R_S}\left(1 - \frac{V_{ocv}}{E_{th}}\right) \qquad (21.)$$

The schematic of the experimental setup of the EMF method is displayed in Figure 4 (b). The pellet-like sample with two electrodes (Pt or Ag) is well attached and sealed to a tube. To generate a concentration cell, gas 1 and gas 2 with different gas components are fed to the outside and inside electrodes, respectively. The open circuit voltages can be measured by a voltmeter or an electrochemical station. Ohmic resistance (R_S) and total resistance (R_T) can be obtained by electrochemical impedance spectroscopy.

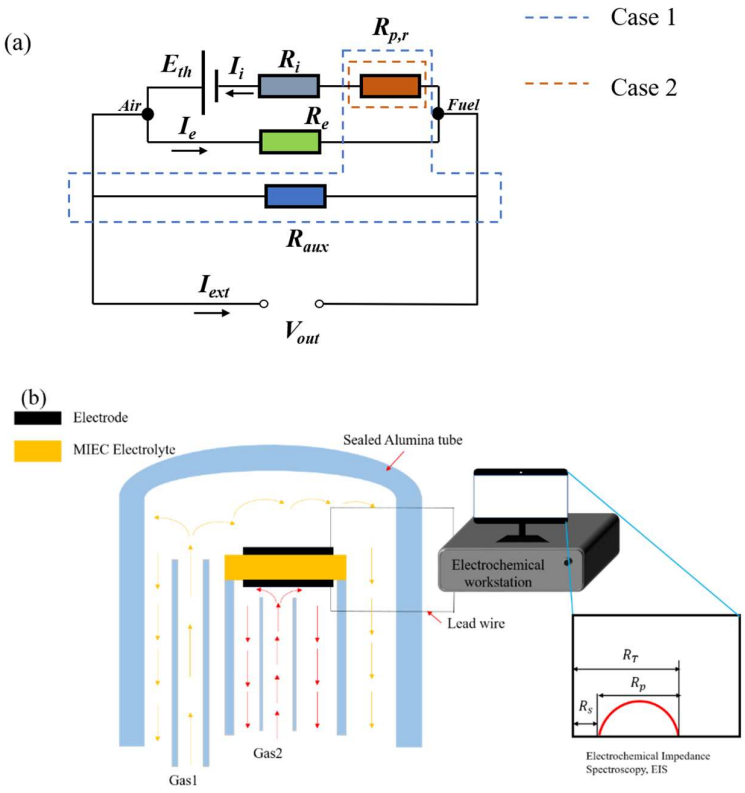

Figure 4 (a) Equivalent circuits for EMF method; (b) schematic of test setup. R_i, $R_{p,r}$, R_e and R_{aux} refer to the ionic resistance, real electrode polarization resistance, electronic resistance in the cell, and external variable resistance, respectively. I_i, I_e and I_{ext} are ionic current, electronic current and external current, respectively.

3.2 The modifications of the EMF method

The assumption of reversible electrodes is adopted in the classical EMF method firstly proposed by Wagner [52]. However, in practice, the electrode polarization cannot be ignored in most cases, and the neglection of electrode polarization will lead to underestimation of the ionic transport number. Wang and Liu *et al.* [53] have reported that the error in determining ionic transport numbers using the ratio of open

circuit voltages to theoretical equilibrium voltages depends sensitively on the electrode polarization resistance as well as the conduction properties of the studied materials. Consequently, the classical EMF method has been modified with considering the electrode polarization resistance by Gorelov [54] in 1988, Liu *et al.* [55] in 1996, and Zhang *et al.* [27] in 2020, as summarized in Table 1.

Table 1 Summary of modification in the EMF method

	Classical[52]	Gorelov modified[54]	Liu modified[55]	Zhang modified[27]
t_i^{app}	$\frac{V_{ocv}}{E_{th}}$	$\frac{R_e}{R_e+R_i}$	$\frac{V_{ocv}}{E_{th}}\left(1+\frac{R_{p,r}}{R_i+R_e}\right)$	$\frac{V_{out}+I_{ext}R_T}{E_{th}}\left(1+\frac{R_{p,r}}{R_i+R_e}\right)$
R_e	$\frac{E_{th}}{V_{ocv}}R_S$	$\frac{A}{B}$	$\frac{R_T}{1-\frac{V_{ocv}}{E_{th}}}$	$\frac{R_T}{1-\frac{V_{out}+I_{ext}R_T}{E_{th}}}$
R_i	$\frac{R_S}{1-\frac{V_{ocv}}{E_{th}}}$	$\frac{R_sR_e}{R_e-R_s}$	$\frac{R_s}{1-\frac{R_s}{R_T}\left(1-\frac{V_{ocv}}{E_{th}}\right)}$	$\frac{R_s}{1-\frac{R_s}{R_T}\left(1-\frac{V_{out}+I_{ext}R_T}{E_{th}}\right)}$
	Neglecting $R_{p,r}$	$\frac{E_{th}}{V_{out}}-1=A\frac{1}{R_{aux}}+B$ $A=R_i+R_{p,r}$, B=$\frac{R_i+R_{p,r}}{R_e}$	Under OCV condition	Under OCV and operating conditions

The principle of Gorelov modified EMF can be illustrated by an equivalent circuit consisting of E_{th}, ionic resistance (R_i) and electronic resistance (R_e) of the MIEC electrolyte, real electrode polarization resistance ($R_{p,r}$) and external variable resistance (R_{aux}), as shown in Figure 4 (a) (case 1). Based on Kirchoff's law, the following expression can be obtained [54]:

$$\frac{E_{th}-V_{out}}{R_i+R_{p,r}}=\frac{V_{out}}{R_e}+\frac{V_{out}}{R_{aux}} \quad (22.)$$

where V_{out} is the output voltage of the cell. Taking R_{aux} as an independent variable, eq. (22) is transformed into [56]:

$$\frac{E_{th}}{V_{out}}-1=(R_i+R_{p,r})\frac{1}{R_{aux}}+\frac{R_i+R_{p,r}}{R_e} \quad (23.)$$

Assuming $(R_i + R_{p,r})$ and R_e are constant at different V_{out}, the plot of $(\frac{E_{th}}{V_{out}} - 1)$ versus $\frac{1}{R_{aux}}$ should be linear with a slope of $(R_i + R_{p,r})$ and an intercept of $\frac{R_i+R_{p,r}}{R_e}$. Thus R_e can be obtained by fitting the linear relationship of eq. (23) [57]. The ohmic resistance (R_S) can be measured by EIS and R_i can be determined according to the following relation:

$$R_s = \frac{R_i R_e}{R_i + R_e} \quad (24.)$$

However, it deserves mentioning that the presumption of constant $(R_i + R_{p,r})$ and R_e may be unreasonable in some conditions. The nonlinear kinetic behavior of the electrode polarization, which can be described by the Butler-Volmer equation, has been well demonstrated [58]. In other words, the real electrode polarization resistance varies with the output voltage, instead of keeping unchanged. The validity of constant electrode polarization resistance has been studied. A criterion proposed to verify the constant electrode polarization resistance is based on the values of dimensionless overpotential $(\frac{F\eta}{RT})$. Nearly constant electrode polarization resistance can be expected when the values of $(\frac{F\eta}{RT})$ remain smaller than approximately 0.2 [56]. Moreover, it has been experimentally demonstrated that the electronic resistance of some MIEC oxides also varies with the output voltage [59]. In the term of theory, the change of the output voltage has an effect on the distribution of charged defects in the MIEC electrolyte, which may considerably influence their electrical conduction properties [60, 61]. Moreover, the MIEC electrolyte, fabricated by conventional ceramic processing technologies, usually shows polycrystalline microstructure. The space charge layer at the grain boundaries of polycrystalline oxides can result in nonlinear electrical

conduction properties, meaning that the resistances are not constant [62, 63]. As a result, there have been some arguments about the use of the Gorelov method [64].

Instead of using external variable resistance (R_{aux}), Liu *et al.* [55] proposed to determine the conduction properties of mixed ionic-electronic oxides by combining AC electrochemical impedance spectroscopy (EIS) and measurement of open circuit voltages (V_{ocv}). The principle of Liu modified EMF method can be elaborated by an equivalent circuit (case 2) shown in Figure 4 (a). According to Kirchoff's law, the following relationship can be obtained under open circuit condiction ($V_{out} = V_{ocv}$):

$$\frac{E_{th}-V_{ocv}}{R_i+R_e} = \frac{V_{ocv}}{R_e} \tag{25.}$$

Combining the definition of ionic transport number and eq. (25), it follows:

$$t_i^{app} = \frac{V_{out}}{E_{th}}\left(1 + \frac{R_{p,r}}{R_i+R_e}\right) \tag{26.}$$

Comparing eqs. (19) and (26), it clearly shows that the influence of electrode polarization resistances on determining ionic transport number. Neglecting electrode polarization resistances leads to underestimated values of the ionic transport number.

The measurement of EIS in Liu modified EMF method is used to determine ohmic resistances (R_S) and total resistances of the cell (R_T), which correspond to the intercepts of the real axis at high frequency and low frequency, respectively, as shown in the Figure 4 (b). R_T is defined as:

$$\lim_{\omega\to 0}\{Z\} = R_T = \frac{(R_i+R_{p,r})R_e}{(R_i+R_{p,r})+R_e} \tag{27.}$$

Combining eq. (24), (25) and (27), R_e and R_i can be calculated as follows:

$$R_e = \frac{L}{\sigma_e} = \frac{R_T}{1-\frac{V_{ocv}}{E_{th}}} \tag{28.}$$

$$R_i = \frac{L}{\sigma_i} = \frac{R_S}{1-\frac{R_S}{R_T}\left(1-\frac{V_{ocv}}{E_{th}}\right)} \tag{29.}$$

It is noteworthy that the Liu modified EMF method is performed under the open circuit condition. This method has been widely applied to characterize the conduction properties of mixed ionic-electronic conducting oxides under the open circuit condition [65]. However, the practical application of MIEC oxides is mostly under operation conditions (under a certain voltage and current), such as solid oxide fuel cells, solid oxide electrolysis cells, and gas pumps. The electrical conduction properties of MIEC oxides may vary under different applied voltages or currents. Hence, the characterization of conduction properties of MIEC oxides under operation conditions is important. The reliability of Liu modified EMF method is questionable under operation conditions.

In 2020, Zhang *et al.* [27] proposed a new EMF method to determine the conduction properties of MIEC oxides under the discharge and electrolysis states. The external current is introduced into the equivalent circuit of the EMF method for considering the variations of cell resistances under operation conditions. Compared with Liu modified EMF method, external current (I_{ext}), ionic current (I_i) and electronic current (I_e) are considered in the equivalent circuit of Zhang modified EMF method, as shown in Figure 4 (a). On the basis of the Kirchhoff's law, the currents and voltages satisfy:

$$I_i + I_e + I_{ext} = 0 \tag{30.}$$

$$V_{out} = E_{th} + I_i\left(R_i + R_{p,r}\right) \tag{31.}$$

$$V_{out} = I_e R_e \tag{32.}$$

Through combining eqs. (1), (27) and (30)-(32) and mathematically transforming, the electrical conduction properties of the mixed ionic-electronic conducting layer can be calculated by the following equations:

$$t_i^{app} = \frac{V_{out}+I_{ext}R_T}{E_{th}}\left(1+\frac{R_{p,r}}{R_i+R_e}\right) \quad (33.)$$

$$R_e = \frac{R_T}{1-\frac{V_{out}+I_{ext}R_T}{E_{th}}} \quad (34.)$$

$$R_i = \frac{R_s}{1-\frac{R_s}{R_T}\left(1-\frac{V_{out}+I_{ext}R_T}{E_{th}}\right)} \quad (35.)$$

Notably, when I_{ext} is equal to 0 (under open circuit condition), the equations of Zhang modified EMF method are identical to those of Liu modified EMF method, indicating that Zhang modified EMF method can be applied under both open circuit and operating conditions. Moreover, it deserves mentioning that during the EIS measurement under operation conditions, relatively large errors may be introduced due to the instability of the system. As a result, the measurement needs to be repeated to avoid system errors. Lastly, an extreme case to note is that when the cell is short-circuited ($V_{out} = 0$), there is no driving force for the electronic current ($I_e = 0$) and the external current is totally due to the ionic current ($I_{ext} = I_i$). In this short-circuited condition, the ionic resistance can be estimated directly according to eq. (31) [66].

The modification of the EMF method is summarized in Table 1. It is clear that except for the classical method, the effect of electrode polarization resistance is taken into account in the other three methods. The Liu modified EMF method is established under the open circuit condition and its reliability under operating conditions is suspectable. The Gorelov and Zhang modified methods are deduced under operation conditions. However, in the Gorelov modified method, the electrical conduction

properties of the MIEC electrolyte are assumed to be independent of output voltages, which isn't reasonable in some cases. By contrast, in the Zhang modified method, the external current is introduced into the equivalent circuit by considering the variations of the conduction properties under operation conditions, suggesting its wide applicability. Lastly, an important point to note is that the EMF method has been developed based on the use of equivalent circuits, in which Ohm′s law is adopted to describe the transport behavior of charge carriers. However, the driving forces to transport charge carriers include not only potential gradient but also concentration gradient [67]. Therefore, instead of the Ohm′s law, the Nernst-Planck equation should be applied [39, 68]. Strictly speaking, the EMF method that has been developed based on the Ohm′s law, isn't completely accurate in theory but may be feasible and operable in practice.

3.3 The case of triple ionic-electronic conducting oxides

In the above discussion about the EMF method, mixed ionic-electronic conducting oxides with only one type of ionic charge carriers have been considered. In this section, the discussion is extended to the cases with two types of ionic charge carriers, especially for oxygen ions and protons. The extension of the original Wagner theory for MIEC oxides to include oxygen ion and proton transport has been developed [69]:

$$V_{ocv} = t_O^{app} \frac{RT}{4F} ln \frac{p''_{O_2}}{p'_{O_2}} + t_H^{app} \frac{RT}{2F} ln \frac{p'_{H_2}}{p''_{H_2}} \quad (36.)$$

During the measurement, the chemical equilibrium between hydrogen, oxygen, and water vapor needs to be taken into account [70]:

$$H_2 + \frac{1}{2} O_2 \rightleftharpoons H_2O \quad (II)$$

$$K_1 = \frac{p_{H_2O}}{p_{H_2} p_{O_2}^{\frac{1}{2}}} \tag{37.}$$

where K_1 is the equilibrium constant of reaction (II). Combing eqs. (36) and (37), eq.(36) can be rewritten as:

$$V_{ocv} = \left(t_O^{app} + t_H^{app}\right) \frac{RT}{4F} ln \frac{p_{O_2}''}{p_{O_2}'} + t_H^{app} \frac{RT}{2F} ln \frac{p_{H_2O}'}{p_{H_2O}''} \tag{38.}$$

$$V_{ocv} = \left(t_O^{app} + t_H^{app}\right) \frac{RT}{2F} ln \frac{p_{H_2}'}{p_{H_2}''} + t_O^{app} \frac{RT}{2F} ln \frac{p_{H_2O}''}{p_{H_2O}'} \tag{39.}$$

On the basis of eqs. (38) and (39), the transport numbers of triple ionic-electronic conducting oxides can be measured by gas concentration cells, namely hydrogen concentration cells, oxygen concentration cells, and water vapor concentration cells [65, 71, 72]. When the steam partial pressures on both sides of the MIEC membrane is kept the same, the second term ($\frac{RT}{2F} ln \frac{p_{H_2O}'}{p_{H_2O}''}$) on the right side of eq. (38) or (39) is equal to zero. As a result, the total apparent ionic transport number ($=t_O^{app} + t_H^{app}$) can be determined by using the hydrogen concentration cells or the oxygen concentration cells. To further identify the contribution of oxygen-ion or proton transport number to the total apparent ionic transport number, the water vapor concentration cells can be employed. When water vapor concentration cells with identical oxygen partial pressures at both sides of the membrane are employed, the first term on the right side of eq. (38) is omitted and t_H^{app} can be determined by the ratio of V_{oc} and $\frac{RT}{2F} ln \frac{p_{H_2O}'}{p_{H_2O}''}$. Analogously, t_O^{app} can be estimated by the ratio of V_{ocv} and $\frac{RT}{2F} ln \frac{p_{H_2O}''}{p_{H_2O}'}$ by applying the water vapor concentration cells with identical hydrogen partial pressures at both sides of the membrane. It is noteworthy that the transport numbers determined using oxygen/hydrogen concentration cells are not exactly equal to those determined by water vapor concentration cells because of different gas atmospheres.

An important point to note is that the influence of electrode polarization resistances isn't taken into account in eqs. (38) and (39). Therefore, it is necessary to make corrections by using the modified EMF methods listed in Table 1. Notably, since the above correction methods are developed from the cases with a single ionic carrier, their suitability in triple ionic-electronic conducting oxides is questionable [70], which requires further investigation. In 2014, Pérez-coll and Mater *et al.* [71] have built some approximate equivalent circuits, including oxygen-ionic resistance (R_O), protonic resistance (R_H) and electronic resistance (R_e), to modify the Gorelov modified EMF method for determining the protonic and oxygen-ionic transport numbers of $SrZr_{0.9}Y_{0.1}O_{3-\delta}$, which is a candidate protonic ceramic electrolyte material. Moreover, it has been reported that for the mixed ionic-electronic conducting oxides with only one type of mobile ion, open circuit voltage is a state function and independent of path and time. However, in the system of triple ionic-electronic conducting oxides, open circuit voltage is path and time-dependent. This can be explained by the fact that open circuit voltage of TIEC membranes is determined by the diffusion paths of the mobile defects. After changing the gas atmospheres, there may remain a residual voltage, representing its history-dependence. The detailed theoretical principles and experimental results can be found in the literature [73, 74]. In other words, open circuit voltage varies as time elapses. Eq. (38) and (39) are valid only at the steady state (time→∞), which should be paid attention to during experimental measurements.

4. Faradaic efficiency (FE) method

4.1 The basic principles of the FE method

The FE method is one of useful experimental methods for determining the ionic transport numbers of materials. It has also been implemented to measure the ionic transport number of mixed ionic-electronic conducting oxides [75, 76]. The basic principle of the FE method can also be illustrated by using an equivalent circuit, as shown in Figure 5 (a). When the chemical potentials of active species between the two electrodes are the same ($E_{th} = 0$) and the electrode polarization resistances are neglected, the following mathematical relationship can be easily obtained based on the Kirchoff's law [77]:

$$t_i = \frac{R_e}{R_e + R_i} = \frac{I_i}{I_{ext}} \tag{40.}$$

It should be noted that because the conduction properties of an MIEC oxide may vary with I_{ext} or V_{out} [76, 78], t_i determined by the FE method can only represent the value under a specific operation condition.

(a)

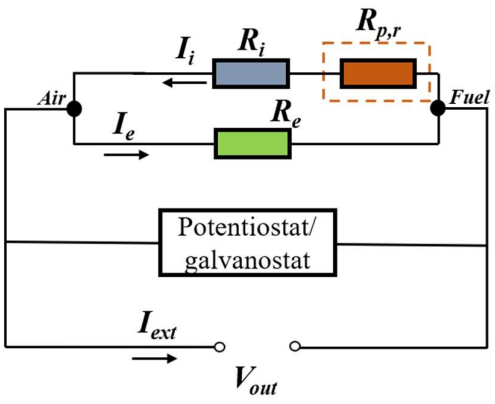

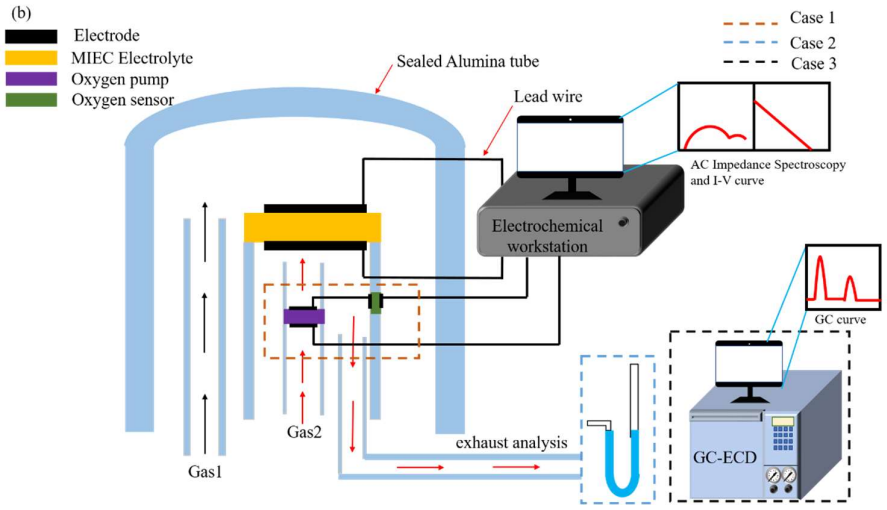

Figure 5(a) Equivalent circuits for the Faradaic efficiency method; (b) schematic of test setup. R_i, $R_{p,r}$, and R_e refer to the ionic resistance, real electrode polarization resistance and electronic resistance in the cell, respectively. I_i, I_e and I_{ext} are ionic current, electronic current and external current, respectively.

The schematic experimental apparatus of the Faradaic efficiency method is displayed in Figure 5(b). Dense membranes of MIEC oxides with two electrodes are attached and sealed to an alumina tube. Gas 1 and gas 2 with identical gas component are fed to both electrodes. The external current (I_{ext}) is measured by an electrochemical workstation or an amperemeter. The critical point of the FE method is the determination of ionic current density (I_i) by accurately measuring the gas flux. Taking oxygen-ionic current as an example ($I_i = I_o$), as shown in Figure 5(b), the combination of oxygen sensor and oxygen pump (case 1) [79], or a standard water-column (case 2) [80], or gas chromatography (case 3) can be used to measure the oxygen flux (J_{o_2}), and the oxygen-ionic current can be calculated ($I_o = 4FJ_{o_2}$). Pure ionic conductors, such as Y_2O_3 stabilized ZrO_2 (YSZ), can be used to evaluate the reliability of the experimental setup

and test procedures. Similarlly, for mixed protonic and electronic conducting oxides ($I_i = I_H$), the protonic current is proportional to the hydrogen flux ($I_H = 2FJ_{H_2}$).

4.2 The modifications of the FE method

Similar to other methods, neglecting the elctrode polarization resistance would lead to incorrect estimation of ionic transport number (t_i). Based on the analysis of the equivalent circuit with elctrode polarization resistance ($R_{p,r}$), as displayed in Figure 5(a), t_i can be estimated by the following formula [78]:

$$t_i = \frac{I_i}{I_{ext}}\left(\frac{R_e+R_i+R_{p,r}}{R_e+R_i}\right) = 1 - \frac{R_s(I_{ext}-I_i)}{V_{out}} \quad (41.)$$

where ohmic resistance (R_s) can be obtained by AC electrochemical impedance spectroscopy. Comparing eq. (40) and (41), it is apparent that when the electrode polarization resistance is significant, applying the classical FE method results in underestimation of ionic transport numbers.

4.3 The case of triple ionic-electronic conducting oxides

Measuring the conduction properties of TIEC oxides by the FE method is also feasible. Geffroy *et al.* [35] have proposed a new setup for the determination of ionic transport numbers (t_O and t_H) of mixed oxygen-ionic and protonic conducting oxides. Assuming the Faraday's law is valid and there is no coupling between oxygen flux (J_{o_2}) and hydrogen flux (J_{H_2}), t_O and t_H can be determined by:

$$t_O = \frac{2J_{o_2}}{2J_{o_2}+J_{H_2}} = \frac{I_o}{I_{ext}} \quad (42.)$$

$$t_H = \frac{J_{H_2}}{2J_{o_2}+J_{H_2}} = \frac{I_H}{I_{ext}} \quad (43.)$$

It deserves mentioning that if water vapor exists in the electrode, a side reaction (reduction of water) and chemical equilibrium of reaction (II) should be carefully taken

into account. The measurement of the generated gas fluxs can be realized by using an gas chromatography or a chilled mirror hygrometer. Accurately simultaneous measurement of different gas percentages is pivotal in calculating the transport properties of TIEC oxides using eqs. (42) and (43).

5. Hebb-Wagner (H-W) method

5.1 The basic principles of the H-W method

The H-W method was developed based on the theory of Wagner [52] and firstly applied to measure the electronic conductivity of silver sulfide by Hebb [81]. To date, the H-W method has been used by many researchers [24, 82] for determining partial electronic conductivities and partial ionic conductivities of MIEC oxides. The unique point of the H-W method is the use of a blocking electrode to suppress the current of one type of charge carriers. Taking the mixed oxygen-ionic and electronic conducting oxide as an example, the basic principle of the H-W method is briefly outlined below. To determine the partial electronic conductivity, an ion-blocking electrode is implemented. Consequently, the ionic current across the MIEC sample is equal to 0 ($I_i = 0$) and the detected external current density (I_{ext}) is equal to the electronic current density (I_e), obeying the Nernst-Planck equation:

$$I_j = -\frac{\sigma_j}{z_j F}\frac{d\tilde{\mu}_j}{dx} \tag{44.}$$

$$I_{ext} = I_e = \frac{\sigma_{e'}}{F}\frac{d\tilde{\mu}_{e'}}{dx} - \frac{\sigma_{h^{\cdot}}}{F}\frac{d\tilde{\mu}_{h^{\cdot}}}{dx} \tag{45.}$$

where $\tilde{\mu}$ is the electrochemical potential, the superscripts of e' and $h^{\cdot}$ represent n-type and p-type electronic defect, respectively. In the MIEC sample, local equilibrium exists:

$$O_2 \rightleftharpoons 2O^{2-} - 4e^- \tag{III}$$

$$\mu_{O_2} = 2\tilde{\mu}_{O^{2-}} - 4\tilde{\mu}_{e'} \tag{46.}$$

$$\frac{d\mu_{O_2}}{dx} = 2\frac{d\tilde{\mu}_{O^{2-}}}{dx} - 4\frac{d\tilde{\mu}_{e'}}{dx} \tag{47.}$$

Becasue $I_i = 0$, according to the Nernst-Planck equation, it is easy to deduce that the gradient of electrochemical potential of oxygen ion is equal to 0 ($\frac{d\tilde{\mu}_{O^{2-}}}{dx} = 0$). Thus eq. (47) is simplified to:

$$\frac{d\mu_{O_2}}{dx} = -4\frac{d\tilde{\mu}_{e'}}{dx} = 4\frac{d\tilde{\mu}_{h^{\cdot}}}{dx} \tag{48.}$$

combining eqs. (45) and (48), then intergrating eq. (45):

$$LI_e = -\frac{1}{4F}\int_{\mu_{O_2}^0}^{\mu_{O_2}^L}(\sigma_{e'} + \sigma_{h^{\cdot}})\, d\mu_{O_2} \tag{49.}$$

where the superscripts of 0 and L represent the interfaces between the MIEC sample and the electrode at the left and right side, respectively, as shown in Figure 6. The measured voltage (V_{out}) between the two electrodes (E_1 and E_4) is proportional to the difference of $\tilde{\mu}_{e'}$ between the two electrodes. Consequently,

$$-FV_{out} = \tilde{\mu}_{e'}^L - \tilde{\mu}_{e'}^0 = -\frac{\mu_{O_2}^L - \mu_{O_2}^0}{4} \tag{50.}$$

According to the definition of the chemical potential, it can be derived:

$$d\mu_{e'} = RTdln[e']_L = -RTdln[h^{\cdot}]_L \tag{51.}$$

where $[X]_L$ is the formula-unit molar concentration of X. Assuming the concentration of oxygen ion is homogeneous within the sample ($\nabla\mu_{O^{2-}} = 0$), it can be derived that the formula-unit molar concentrations of e' and $h^{\cdot}$ are proportional to $P_{O_2}^{-\frac{1}{4}}$ and $P_{O_2}^{\frac{1}{4}}$ respectively [83, 84]. By integrating eq. (51),

$$[e']_L = exp\left[-\frac{\mu_{O_2} - \mu_{O_2}^0}{4RT}\right][e']_L^0 \tag{52.}$$

$$[h^{\cdot}]_L = exp\left[\frac{\mu_{O_2} - \mu_{O_2}^0}{RT}\right][h^{\cdot}]_L^0 \tag{53.}$$

The defect conductivity is proportional to the defect concentration ($\sigma_k \propto [k]_L$). Combining eqs. (49), (50), (52) and (53), then integrating eq. (49):

$$I_e = -\frac{RT}{FL}\left[\left(1 - exp\left(-\frac{FV_{out}}{RT}\right)\right)\sigma_{e'}^0 + \left(exp\left(\frac{FV_{out}}{RT}\right) - 1\right)\sigma_{h^\cdot}^0\right] \qquad (54.)$$

eq. (54) is the standard equation of the H-W method for determining electronic conductivity of MIEC oxides [24, 83, 85]. Through fitting the current-voltage relationship by using eq. (54), $\sigma_{e'}^0$,$\sigma_{h^\cdot}^0$ and total electronic conductivity ($\sigma_e = \sigma_{e'} + \sigma_{h^\cdot}$) can be obtained. Notably, the current should be measured at steady states.

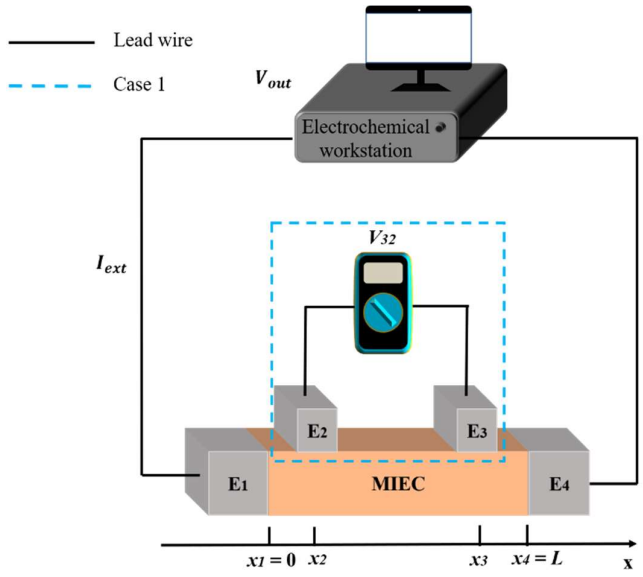

Figure 6 Schematic of the Hebb-Wagner method

The experimental setup of the H-W method is shown schematically in Figure 6. It consists of a reversible electrode (E_1), an MIEC sample, a blocking electrode (E_4), and an electrochemical workstation. When the partial electronic conductivity is measured, E_4 is implemented as the ion-blocking electrode, possessing negligible ionic conductivity as low as possible but considerably high electronic conductivity. In order to prevent any oxygen exchange reactions with the gaseous atmosphere at the ion-

blocking electrode, the entire surface of the ion-blocking electrode has to be covered by glass [82]. A micro-electrode can be used as an ion-blocking electrode, which facilitates the sealing of the electrode and reduces the relaxation time towards the steady state [85, 86].

5.2 The modifications of the H-W method

The standard H-W equation isn't valid in all conditions. Riess [24] has comprehensively reviewed the limitation of the standard H-W method. High applied voltage, variable charge ionic defects, non-ideal ion-blocking electrode, decomposition of the sample, non-negligible electrode overpotentials or contact resistances can lead to failure of the standard H-W method.

Table 2 Summary of modification in the H-W methods

	Type	Basic equation
Measurement of σ_e	Standard [24]	$I_e = -\frac{RT}{FL}\left[\left(1 - exp\left(-\frac{FV_{out}}{RT}\right)\right)\sigma_{e'}^{0} + \left(exp\left(\frac{FV_{out}}{RT}\right) - 1\right)\sigma_{h^{\cdot}}^{0}\right]$
	Guo and Maier modified [87]	$I_e = -\frac{RT}{FL}\left[\left(1 - exp\left(-\frac{\alpha FV_{out}}{RT}\right)\right)\sigma_{e'}^{0} + \left(exp\left(\frac{\alpha FV_{out}}{RT}\right) - 1\right)\sigma_{h^{\cdot}}^{0}\right]$
	Four-probe method [88] (E_1 is reversible, $E_{2,3,4}$ are ion-blocking)	n-type σ_e dominates: $e^{-\frac{qV_{32}}{kT}} = \frac{kT\sigma_n + x_3 q l_{e^-}}{kT\sigma_n + x_2 q l_{e^-}}$ p-type σ_e dominates: $e^{-\frac{qV_{32}}{kT}} = \frac{kT\sigma_p + x_3 q l_{e^-}}{kT\ _p + x_2 q l_{e^-}}$

	Four-probe method [88] (E_2 is reversible, $E_{1,3,4}$ are ion-blocking)	$I_e = -\frac{RT}{FL_{32}}\left[\left(1-exp\left(-\frac{FV_{32}}{RT}\right)\right)\sigma_{e'}^{2} + \left(exp\left(\frac{FV_{32}}{RT}\right)-1\right)\sigma_{h^{\cdot}}^{2}\right]$
Measurement of σ_i	Standard [24]	$\sigma_i = \frac{LI_{ext}}{V_{out}}$

Because of the above restrictions of the standard H-W method, some modifications have been made to improve the applicability of the H-W method, as summazied in Table 2. At relatively high applied voltages, the assumption of uniform distribution of mobile ionic defect ($\nabla\mu_i = 0$) within the mixed ionic-electronic samples does not hold. Hence, Riess [89] has deduced new mathematical I-V relationships of the H-W method. To solve the problems of the assumption of $\nabla\mu_i = 0$, Guo and Maier [87] have introduced the coefficient α to modify the standard H-W equation and a generalized equation is obtained:

$$I_e = -\frac{RT}{FL}\left[\left(1-exp\left(-\frac{\alpha FV_{out}}{RT}\right)\right)\sigma_{e'}^{0} + \left(exp\left(\frac{\alpha FV_{out}}{RT}\right)-1\right)\sigma_{h^{\cdot}}^{0}\right] \qquad (55.)$$

where $\alpha = 4|N|$ for oxides and N is the characteristic exponent in $\sigma_{h^{\cdot}} \propto \sigma_{e'}^{-1} = P_{O_2}^{|N|}$. α is not a constant and may vary with oxygen activity, especially at high temperatures [90]. However, when there is a redox active dopant in the mixed ionic-electronic conducting oxides, such as Pr^{3+}/Pr^{4+} in $Ce_{0.8}Pr_{0.2}O_{2-\delta}$, the I-V curves can't be described adequately by eq. (54) or (55). The H-W equation has to be modified by considering the presence of redox active dopants, making it complicated [85].

Similar to the EMF and FE methods, neglecting electrode overpotentials can lead to underestimation in the measured partial conductivities [84]. To exclude the influence

of non-negligible electrode overpotentials and contact resistances, various approaches have been developed [84]. Dudley *et al.* [91] and Riess [88] have proposed a 4-probe configuration to replace the standard 2-probe configuration. As shown in case 1 of Figure 6, two additional voltage probes (E_2 and E_3) situated at a known distance are employed to measure the voltage drop. Both E_2 and E_3 are ion-blocking electrodes. When the n-type electronic conductivity is dominant, the electronic conductivity and measured voltages satisfy [88]:

$$exp\left(-\frac{FV_{32}}{RT}\right) = \frac{RT\sigma_{e'}^{0} - FL_{32}I_e}{RT\sigma_{e'}^{0} - FL_{32}I_e} \tag{56.}$$

where V_{32} and L_{32} are the voltage difference and length between electrode E_2 and E_3, respectively. Similarly, when the p-type electronic conductivity is dominant, the electronic conductivity and measured voltages satisfy [88]:

$$exp\left(\frac{FV_{32}}{RT}\right) = \frac{RT\sigma_{h^{\cdot}}^{0} - FL_{32}I_e}{RT\sigma_{h^{\cdot}}^{0} - FL_{32}I_e} \tag{57.}$$

There is another configuration of 4-probe method, in which E_2 is revsersible and electrodes $E_{1,2,4}$ are ion-blocking. In this configuration, because on current is flowing through electrode E_2, $\sigma_{e'}^{2}$ or $\sigma_{h^{\cdot}}^{2}$-μ_i relation is not affected by deviation from ideality of electrode E_2. The eletronic conductivity ($\sigma_{e'}^{2}$ and $\sigma_{h^{\cdot}}^{2}$) at x2 position can be evaluated by the following equation [88]:

$$I_e = -\frac{RT}{FL_{32}}\left[\left(1 - exp\left(-\frac{FV_{32}}{RT}\right)\right)\sigma_{e'}^{2} + \left(exp\left(\frac{FV_{32}}{RT}\right) - 1\right)\sigma_{h^{\cdot}}^{2}\right] \tag{58.}$$

Besides the bar-type sample, the 4-probe method can be applied to cylindrical samples, like the van der Pauw electrode configuration [88]. In 2018, an in-plane geometrical configuration has been proposed in the 2-probe H-W method, as shown in Figure 7. Because the contribution of the electrode overpotential to the total resistance can be

neglected in this geometry, so the measured results by the 2-probe method are in good agreement with those measured by the 4-probe method. This result suggests that the in-plane geometry in the H-W method is better than the bulk geometry in terms of eliminating the influence of the electrode overpotential.

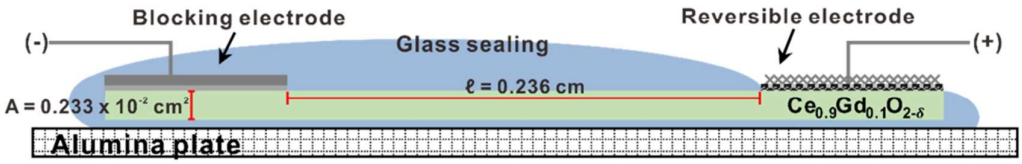

Figure 7 Schematic view of a thick-film polarization cell in plane geometry [82].

Besides determining partial electronic conductivity (σ_e), the H-W method can be extended to estimate the partial ionic conductivity (σ_i) with the use of an electron-blocking electrode, instead of an ion-blocking electrode. The ratio between the applied voltage and external current density yields the ionic resistance of the mixed ionic-electronic conducting sample [24]:

$$R_i = \frac{L}{\sigma_i} = \frac{V_{out}}{I_{ext}} \tag{59.}$$

However, eq. (59) can be applied only under restrictive conditions. Similar to determination of the partial electronic conductivity by the standard H-W method, high applied voltages, variable charge ionic defects, non-ideal electron-blocking electrode, decomposition of the sample, non-negligible electrode overpotentials or contact resistances can lead to failure of eq. (59) [24]. The effect of non-negligible electrode overpotentials or contact resistances can be avoided by applying the 4-probe test configuration. Sadadi and Riess [92] have also proposed a modified 4-probe H-W method for simultaneously measuring ionic and electronic conductivities. This method

is tested experimentally on the solid electrolyte CuBr. However, this method has never been applied to mixed ionic-electronic conducting oxides. Therefore, the feasibility of this method in MIEC oxides deserves further study. Moreover, introducing a porous electrode between the MIEC sample and the electron-blocking electrode can prevent the problems of non-negligible interface polarization resistance and possible reduction of the electron-blocking electrode, which can lead to leakage of electronic current [93, 94].

5.3 The case of triple ionic-electronic conducting oxides

The H-W method has also been implemented for measuring the partial conductivities of triple ionic-electronic conducting oxides [51, 95, 96]. Until now, the H-W method is mainly used for determining the electronic conductivity of triple ionic-electronic conducting oxides. For determining electronic conductivity, the principle and experimental setup, mentioned above, can be adopted directly in the cases of triple ionic-electronic conducting oxides. Moreover, theoretically, the oxygen ionic conductivity and protonic conductivity can be distinguished by H-W method. The main challenge is the selection of pure oxygen ionic conductors or pure protonic conductors as the blocking electrodes. YSZ is considered an almost pure oxygen ionic conductor, making it ideal to be blocking electrodes.

6. Gas permeation (GP) method

6.1 The basic principles of the GP method

Determination of partial conductivities of mixed ionic-electronic conducting oxides through the gas permeation method relies on the establishment of mathematical

relationships between the partial conductivity and gas permeation flux. The basic model of gas permeation method was also developed from Wagner's theory [97]. Here, a mixed oxygen-ionic and electronic conductor is taken as an example to illustrate the basic principle. As shown in Figure 8(a), the oxygen permeation flux (J_{O_2}) is chemically driven by the gradient of the oxygen partial pressure imposed across the membrane. There are two adopted assumptions in this model: the surfaces of MIEC oxides on both sides are at equilibrium with the imposed gas atmosphere ($P'_{O_2} = P^{t1}_{O_2}\ and\ P''_{O_2} = P^{t2}_{O_2}$) and the existence of a local equilibrium within the membrane ($O_2 \rightleftharpoons 2O^{2-} - 4e^-$). Under steady state, to maintain charge neutrality, the oxygen-ionic current (I_o) is compensated by the electronic current (I_e) within the membrane and there is no net external current ($\sum_{i=1}^{n} z_i J_i = 0$):

$$I_{ext} = I_o + I_e = -\frac{J_{O^{2-}}}{2F} - \frac{J_{e'}}{F} = \frac{\sigma_o}{2F}\frac{d\tilde{\mu}_{O^{2-}}}{dx} + \frac{\sigma_{e'}}{F}\frac{d\tilde{\mu}_{e'}}{dx} = 0 \qquad (60.)$$

Combining the local equilibrium of reaction (III), it can be derived:

$$J_{O^{2-}} = -\frac{\sigma_o \sigma_{e'}}{8(\sigma_o + \sigma_{e'})F^2} \cdot \frac{\partial \mu_{O_2}}{\partial x} \qquad (61.)$$

According to $J_{o_2} = \frac{1}{2} J_{O^{2-}}$ and $\mu_{O_2} = \mu^0_{O_2} + RTlnP_{O_2}$, then integrating, eq. (61) can be transformed to:

$$J_{O_2} = -\frac{RT}{16\ ^2L}\int_{ln\ \ '_{O_2}}^{lnP''_{O_2}} \frac{\sigma_o \sigma_{e'}}{(\sigma_o + \sigma_{e'})} dln\, P_{O_2} = -\frac{RT}{16\ ^2L}\int_{lnP'_{O_2}}^{ln\ \ ''_{O_2}} \sigma_{tot} t_o t_e dln\, P_{O_2} \qquad (62.)$$

Eq. (62) is the classical model for describing the behavior of oxygen permeation [11]. For the MIEC oxides with predominant electronic conductivity ($t_e \approx 1$), eq. (62) is transformed to:

$$J_{O_2} = -\frac{RT}{16F^2L}\int_{ln\ \ '_{O_2}}^{lnP''_{O_2}} \sigma_o dln\, P_{O_2} \qquad (63.)$$

Under not very high gradient of P_{O_2}, σ_o could be assumed to be constant across the membrane. Thus, eq. (63) can be simplified to:

$$J_{O_2} = -\frac{RT\sigma_o}{16F^2L}\ln\left(\frac{P''_{O_2}}{P'_{O_2}}\right) \tag{64.}$$

On the contrary, in the case of mixed ionic-electronic conducting oxides with predominant oxygen-ionic conduction ($t_o \approx 1$), eq. (62) is simplified to:

$$J_{O_2} = -\frac{RT}{16F^2L}\int_{lnP'_{O_2}}^{lnP''_{O_2}} \sigma_{e'} dln\, P_{O_2} \tag{65.}$$

For n-type electronic conductivity, it is usually proportional to $P_{O_2}^{-\frac{1}{4}}$. Thus eq. (65) is transformed to:

$$J_{O_2} = -\frac{RT\sigma^{\theta}_{e'}}{4F^2L}\left(P''_{O_2}{}^{-\frac{1}{4}} - P'_{O_2}{}^{-\frac{1}{4}}\right) \tag{66.}$$

where $\sigma^{\theta}_{e'}$ is the electronic conductivity at $P_{O_2} = 1\ atm$.

Similarly, for mixed protonic and electronic conducting oxides (Figure 8 (b)), the hydrogen permeation flux (J_{H_2}) is chemically driven by the gradient of the hydrogen partial pressure imposed across the membrane. When the minor defects are protons ($\sigma_H \ll \sigma_e$), the equation for describing the hydrogen permeation is [35, 98]:

$$J_{H_2} = -\frac{RT}{4F^2L}\int_{lnP'_{H_2}}^{lnP''_{H_2}} \sigma_H dln\, P_{H_2} \tag{67.}$$

When the protonic conductivity is predominant ($\sigma_H \gg \sigma_e$), the hydrogen fluxes are limited by the electronic conductivity of the MIEC membrane and obey the following equation:

$$J_{H_2} = -\frac{RT}{4F^2L}\int_{ln\ '_{H_2}}^{ln\ ''_{H_2}} \sigma_e dln\, P_{H_2} \tag{68.}$$

According to eq. (63) - (68), the conductivity of minor defect of mixed ionic-electronic conducting oxides can be determined by measuring the gas permeation flux across the membranes.

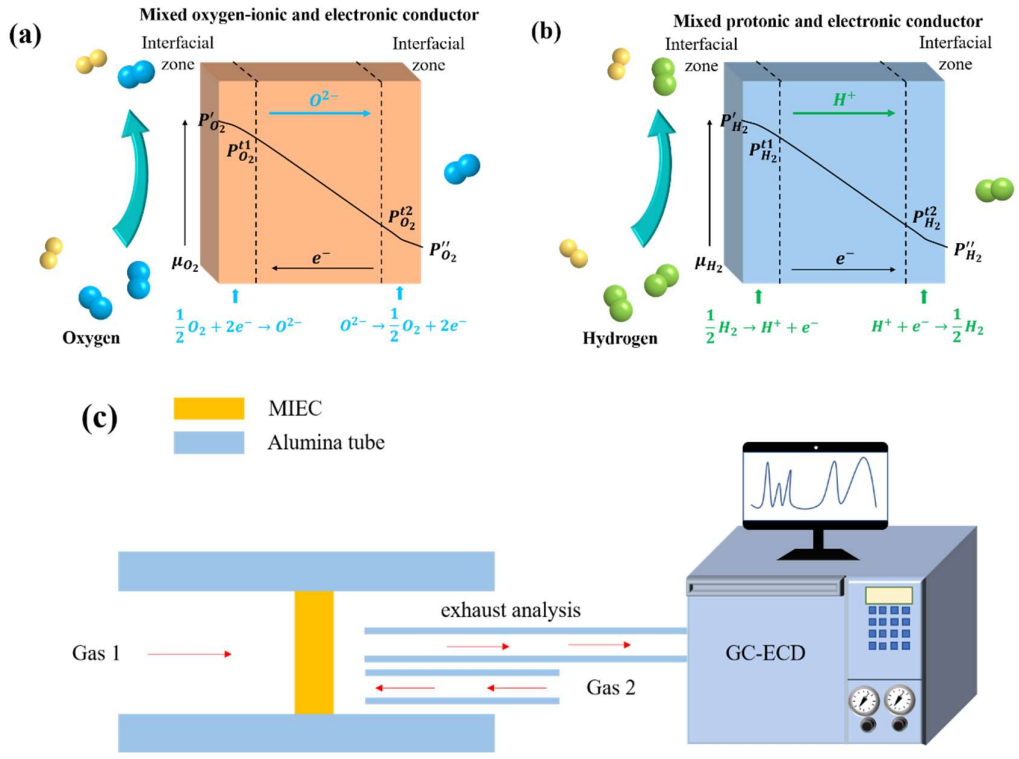

Figure 8 (a) Schematic of gas permeation through mixed oxygen-ionic and electronic conductors; (b) schematic of gas permeation through mixed protonic and electronic conductors; (c) schematic of experimental setup for gas permeation method.

The experimental setup of the gas permeation method is schematically shown in Figure 8(c). To prevent gas leakage, the mixed ionic-electronic conducting membrane should be dense and a good sealing at the edge is required. Gas 1 and 2 with exactly known gas compositions are fed to different sides of the membrane. Similar to the FE method, accurate measurement of the change of gas composition is critical for the GP method. The composition of the exhaust gas is usually analyzed by gas chromatography (GC). Then the gas permeation flux can be evaluated based on the change of gas composition.

6.2 The modifications of the GP method

In the classical model of gas permeation, it is assumed that both surfaces of the membrane remain in equilibrium with the gas phase. This assumption may not hold in practice. As shown in Figure 8 (a), there are interfacial zones on both sides of the membrane and a gradient of P_{O_2} exists in the interfacial zones [99]. Thus, by replacing P_{O_2} with $P_{O_2}^t$, eq. (62) is modified to:

$$J_{O_2} = -\frac{RT}{16F^2L}\int_{lnP_{O_2}^{t1}}^{ln\ P_{O_2}^{t2}} \sigma_{tot} t_o t_e d ln\, P_{O_2} \tag{69.}$$

where $P_{O_2}^{t1}$ and $P_{O_2}^{t2}$ are the actual oxygen partial pressure on the surfaces of the membrane. The actual oxygen partial pressure can be measured using metallic and ceramic point electrodes [35].

In the above discussion, the gas permeation is assumed to be contrlled by bulk diffusion. However, the gas permeation rate through MIEC membrane can be limited by either bulk diffusion or surface exchange reaction, which has been widely recognized [100, 101]. Joo and Yu *et al.*[102] proposed a modified Wagner equation to describe the oxygen permeation flux under mixed bulk diffusion and surface exchange kinetics regime:

$$J_{O_2} = -\frac{RT}{16F^2L(1+2\frac{L_c}{L})}\int_{lnP_{O_2}^{t1}}^{lnP_{O_2}^{t2}} \sigma_{tot} t_o t_e d ln\, P_{O_2} \tag{70.}$$

$$L_c = \frac{D_o}{k} \tag{71.}$$

where L_c is the characteristic thickness and k is the surface exchange coefficient. The value of L_c could represent the relative impact of the bulk diffusion to the exchange reaction. The modification by introducing L_c in eq. (70) is only feasible for cases whereby the oxygen partial pressure gradient across the MIEC membrane is relatively

small or when the surface exchange kinetics are equivalent on both sides of the membrane [100]. With considering the influence of surface exchange kinetics, various gas permeation models, which have been developed by researchers [11, 103], become complicated. These complicated models incorporate the parameters of conduction properties and kinetics of surface exchange reactions, which make it difficult to straightforwardly evaluate the electrical conduction properties of mixed ionic-electronic conducting oxides. Therefore, these gas permeation models are beyond the scope of discussion in this review. To mitigate the impact of surface exchange reactions, two feasible approaches can be applied: increasing the membrane thickness and improving the kinetics of surface exchange reactions with some catalytic-active agents. It is noteworthy that according to the models that are limited by the bulk diffusion, gas permeation is proportional to the reciprocal of the membrane thickness, which can be used as evidence for demonstrating bulk diffusion controlled gas permeation.

6.3 The case of triple ionic-electronic conducting oxides

Also based on Wagner's theory, the models of gas permeation for triple ionic-electronic conducting membranes have been developed by Norby and Larring [104]:

$$J_{O_2} = \frac{-RT}{16F^2L}\int_{P'_{O_2}}^{P''_{O_2}} \sigma_{tot} t_O (t_e + t_H) dlnP_{O_2} + \frac{-RT}{8F^2L}\int_{P'_{H_2}}^{P''_{H_2}} \sigma_{tot} t_O t_H dlnP_{H_2} \quad (72.)$$

$$J_{H_2} = \frac{-RT}{8F^2L}\int_{P'_{O_2}}^{P''_{O_2}} \sigma_{tot} t_H t_O dlnP_{O_2} + \frac{-RT}{4F^2L}\int_{P'_{H_2}}^{P''_{H_2}} \sigma_{tot} t_H (t_e + t_O) dlnP_{H_2} \quad (73.)$$

Eqs. (72) and (73) can be simplified to eqs. (62)-(68) when only one ionic charge carrier is considered. Moreover, it can be found that on the right side of eqs. (72) and (73), there are two terms, namely corresponding to oxygen gradient and hydrogen gradient, contributing to the total gas permeation flux. To straightforwardly determine the

electrical conduction properties of triple ionic-electronic conducting oxides, one of two terms needs to be excluded. Therefore, in the experiment, the oxygen gradient and hydrogen gradient between two sides of the MIEC membrane should be well controlled, which is similar to the cases of hydrogen concentration cells and oxygen concentration cells described in the EMF method.

7. Comparison and combination of different methods

7.1 The range of applications of different methods

Table 3 The applicability of different methods

	Total conductivity measurement	Electromotive force method method	Faradaic efficiency method	Hebb-Wagner method	Gas permeation method
Determination of ionic conductivity	Yes	Yes	No	Yes	Yes
Determination of electronic conductivity	Yes	Yes	No	Yes	Yes
Determination of transport numbers	Yes	Yes	Yes	Yes	No
Open circuit condition	Yes	Yes	No	No	Yes
Operation condition	Yes	Yes	Yes	Yes	No
For TIEC oxides	Yes	Yes	Yes	Yes	Yes

The range of applications of various methods is summarized and compared in six aspects, as shown in Table 3. The partial conductivities of mixed ionic-electronic conducting oxides cannot be directly estimated by the FE method without EIS measurement. Except for the FE method, the other four methods are available to measure the ionic and electronic conductivities of MIEC oxides. There are a few key considerations for these four methods. For the total conductivity measurement, no electrode polarization needs to be taken into account. However, because the conduction properties are determined by the fitting process, the multi-mathematical solutions

should be carefully dealt with. The investigated material is required to remain chemically or physically stable in a sufficiently large range of oxygen partial pressure. The partial conductivities obtained by the EMF method are the apparent partial conductivities representing mean values of the conductivity distribution across the electrolyte layers. For evaluating relatively low ionic conductivity, large errors may be introduced by employing either the total conductivity measurement or the EMF method. On the other hand, the H-W and GP methods allow the accurate determination of low ionic conductivity. For assessing electronic conductivity, the H-W method is more sensitive than the other methods. As for the gas permeation method, only the partial conductivity of minor defects can be evaluated. As a result, this approach is only suitable for the MIEC oxides possessing one predominant conductivity. In the aspect of estimating transport numbers, except for the GP method, the other four methods are applicable. Similar to the partial conductivities, the calculated transport numbers by EMF are the apparent ones. For the H-W method, in order to calculate the transport numbers, the ionic and electronic conductivities can be measured individually or simultaneously. The modified 4-probe H-W method could be applied for the simultaneous measurement.

In terms of test conditions, the conduction properties of MIEC oxides both at open circuit condition and operation condition (under applied voltage/current) need to be evaluated. It has been reported that the conduction properties of MIEC oxides could change significantly under applied voltage/current [59]. According to the models of charged defects distribution in MIEC membranes, the applied voltage/current could

influence the distribution of charged defects in the MIEC membranes, which further affects their electrical conduction properties [60]. Moreover, the tested MIEC samples, fabricated by conventional ceramic processing technologies, usually show polycrystalline microstructure. The space charge layer at the grain boundaries of polycrystalline oxides could lead to nonlinear electrical conduction behaviors, meaning that the resistances vary with the applied voltage/current [62, 63]. From Table 3, it can be found that the FE and H-W methods cannot be conducted at open circuit conditions due to the fact that applied voltages need to be implemented during the test of these two methods. In terms of operation conditions, among these five methods, only the GP method isn't applicable. Despite the fact that the other four methods can be employed at operation conditions, there are limited researches concerning the determination of conduction properties under applied voltage or current [27, 59]. The impact of applied voltage/current on the conduction properties of MIEC oxides needs more investigation. It should be noted that under the applied voltage/current, the test system may become unstable, which is an obstacle to precisely measuring the experimental data.

Although the conduction properties of triple ionic-electronic conducting oxides could be evaluated by these five approaches, correctly estimating the conduction properties remains difficult. The basic formulas of these five methods are summarized in Table 4. Since the partial electrical conductivities are influenced by not only the oxygen partial pressure but also the water partial pressure, the total conductivity measurement can be conducted at various oxygen partial pressures as well as water partial pressures to obtain experimental data for fitting. Even so, when considering

constraints of site conservation and local charge neutrality, it is not easy to unambiguously determine a complete set of conduction properties due to the existence of multiple mathematical solutions. Thermogravimetric analysis, conductivity relaxation measurement, and other methods can provide additional information about defect concentrations, which can reduce the uncertainty of fitting. The formulas of the EMF method listed in the table are without considering the influence of electrode polarization. When the electrode polarization is significant, modifications of the EMF method have to be made and investigated. Moreover, in the case of triple ionic-electronic conducting oxides, open circuit voltage is no longer a state function and it is path and time-dependent. These two equations are valid only at the steady state (time→ ∞), which should be paid attention to during experimental measurements [73, 74]. As for the EMF and GP methods, different types of gas concentration cells are needed to separate the oxygen-ionic and protonic conduction. Precisely controlling the gas composition of the gas concentration cells is required. Avoiding gas leakage and accurately simultaneous measurement of different gas percentages in the exhaust gas are pivotal for the FE and GP methods. To data, the H-W method has been used to evaluate the electronic conductivity of TIEC oxides [51]. Though it is theoretically feasible, the H-W method hasn't been applied to distinguish the oxygen-ionic and protonic conductivities. Selecting pure oxygen ionic conductors or pure protonic conductors as the blocking electrodes is critical. Lastly, the chemical stability of TIEC oxides under test conditions, especially in reducing environments, should be considered.

Table 4 Measurement of conduction properties of triple ionic-electronic conducting oxides

Method	Basic Formulas
Total conductivity measurement [33, 34]	$\sigma_{tot} = \sigma_o + \sigma_H + \sigma_e$
Electromotive force method [69]	$V_{ocv} = \left(t_O^{app} + t_H^{app}\right)\frac{RT}{4F} ln\frac{p''_{O_2}}{p'_{O_2}} + t_H^{app}\frac{RT}{2F} ln\frac{p'_{H_2O}}{p''_{H_2O}}$ $V_{ocv} = \left(t_O^{app} + t_H^{app}\right)\frac{RT}{2F} ln\frac{p'_{H_2}}{p''_{H_2}} + t_O^{app}\frac{RT}{2F} ln\frac{p''_{H_2O}}{p'_{H_2O}}$
Faradaic efficiency method [35]	$t_O = \frac{I_o}{I_{ext}} = \frac{4FJ_{O_2}}{I_{ext}}$, $t_H = \frac{I_H}{I_{ext}} = \frac{2FJ_{H_2}}{I_{ext}}$
Hebb-Wagner method [24]	$I_e = -\frac{RT}{FL}\left[\left(1 - exp\left(-\frac{FV_{out}}{RT}\right)\right)\sigma_{e'}^0 + \left(exp\left(\frac{FV_{out}}{RT}\right) - 1\right)\sigma_{h^{\cdot}}^0\right]$ $R_{O/H} = \frac{L}{\sigma_{O/H}} = \frac{V_{out}}{I_{ext}}$
Gas permeation method [104]	$J_{O_2} = \frac{-RT}{16F^2L}\int_{P'_{O_2}}^{P''_{O_2}} \sigma_{tot}t_O(t_e + t_H)dlnP_{O_2} + \frac{-RT}{8F^2L}\int_{P'_{H_2}}^{P''_{H_2}} \sigma_{tot}t_O t_H dlnP_{H_2}$ $J_{H_2} = \frac{-RT}{8F^2L}\int_{P'_{O_2}}^{P''_{O_2}} \sigma_{tot}t_H t_O dlnP_{O_2} + \frac{-RT}{4F^2L}\int_{P'_{H_2}}^{P''_{H_2}} \sigma_{tot}t_H(t_e + t_O)dlnP_{H_2}$

7.2 The combination of different methods

As mentioned in the above discussion, each method has its limitations. In order to accurately and comprehensively evaluate the conduction properties of mixed ionic-electronic conducting oxides, especially for triple ionic-electronic conducting oxides, it is recommended to combine different methods. To overcome the problem of fitting uncertainty in total conductivity measurement, the partial electronic conductivity can be measured by the H-W method [51, 95]. The partial ionic conductivity can be evaluated by the gas permeation method, when the ionic conductivity is much smaller

than the electronic conductivity [105]. Moreover, evaluating electrical conduction properties at operation conditions is challenging. Since the development of EMF method for operation conditions is based on the model of equivalent circuits, its accuracy at operation conditions deserves further evaluation or modification. Notably, unlike the EMF method, the transport number, evaluated by the aforementioned FE method, does not have a gradient of chemical potential between two sides of the membrane. Hence, the comparison of results obtained by the FE and EMF methods should consider the influence of gas composition and applied voltage/current on the conduction properties [106]. When chemical potential difference between two sides of the membrane exists, the FE method needs to be modified considering the gas flux driven by the chemical potential gradient, which is a combination of the FE method and GP method [107].

Finally, it is noteworthy that all these methods are originated from defect chemistry and Wagner's theory. The key difference between these methods is that the electrical conduction properties of MIEC oxides are evaluated by experimentally measuring different types of data, such as resistance, voltage, current, and gas composition. Measuring these data may involve experimental errors, which are caused by gas leakage through seals, temperature gradients, or high thermo-emf [78]. Carefully considering the principles and applicability, and comparing the results obtained by different methods may be beneficial to mitigate the errors introduced by measuring only one kind of data.

8. Summary and Outlook

Serving as a bridge for researcher entering the field of mixed ionic-electronic oxides, this review article covers five most widely used approaches for estimating their electrical conduction properties, namely total conductivity measurement, electromotive force method, Faradaic efficiency method, Hebb-Wagner method, and gas permeation method. All these methods are initially developed based on defect chemistry and Wagner's theory, and are further improved by considering different influencing factors, such as local charge neutrality, electrode polarization, surface kinetics, applied voltage/current, and so on. Though these five methods have been modified and improved, there are still a number of issues that need to be resolved/clarified:

(1) For total conductivity measurement, when site conservation and local charge neutrality are taken into account, the problem of multi-mathematical solution in fitting needs to be addressed, especially for TIEC oxides. The problem of multi-mathematical solution in fitting can be alleviated by combining total conductivity measurement and other methods, such as the H-W method, the GP method, measurement of transient conductivity (ECR method), thermogravimetric analysis and coulometric titration.

(2) The partial conductivities and transport numbers measured by the EMF method are apparent values under a given gradient of active species. The relationship between these apparent values and the real ones should be studied in the future. Furthermore, the diffusion of charged defects in an MIEC membrane should be described by using the Nernst-Planck equation, rather than the Ohm′s law. Therefore, the modified EMF methods, developed based on ohmic law, aren't completely perfect in theory but are

feasible and operable in practice. Their accuracy in different test conditions deserves further investigation.

(3) Until now, most studies about the electrical conduction properties of MIEC oxides are focused under the open circuit condition. However, the application of MIEC oxides is usually under applied voltage and current. The applied voltage and current can affect the distribution of charged defects across the membrane or the space charge layer at the grain boundaries, resulting in a noticeable change of electrical conduction properties. The use of electrical conduction properties measured at open circuit conditions to predict the conduction behavior at operation conditions may be improper and lead to some problems. Therefore, more research efforts are needed to study the electrical conduction properties under operation conditions. Notably, under the applied voltage and current, the test system may become unstable, which makes it difficult to correctly measure the experimental data.

(4) For triple ionic-electronic conducting oxides, it is difficult to clearly separate the conduction contributed by each charge carrier. Although these five methods are applicable for TIEC oxides, error may be introduced due to some approximate treatment or the complicated test procedure. A relatively simple and reliable strategy needs to be established in the future. Efficiently combining different methods may be feasible.

(5) Though the methods discussed in this paper are primarily for MIEC oxides with oxygen-ionic/protonic conduction, some of these methods with proper modification are also available for MIEC materials conducting other ions, such as Li^+. Recently, the attempts to employ MIEC materials in lithium batteries are growing [108-110].

Properly measuring the partial conductivities of mixed lithium-ionic and electronic conductors is necessary. It has been reported the lithium-ionic conductivity and electronic conductivity can be determined separately by using an electron/ion-blocking electrode [111, 112], which is similar to the H-W method. In short, some basic principles of measuring the conduction properties of MIEC oxides, introduced in this review, can be extended to the mixed lithium-ionic and electronic conducting materials, which requires more research effort.

Acknowledgements

This work was primarily supported by the National Natural Science Foundation of China (Grant No.: 52002082) and the U.S. National Science Foundation (DMR-1832809).

Reference:

[1] G. Chen, A. Feldhoff, A. Weidenkaff, C. Li, S. Liu, X. Zhu, J. Sunarso, K. Huang, X.Y. Wu, A.F. Ghoniem, W. Yang, J. Xue, H. Wang, Z. Shao, J.H. Duffy, K.S. Brinkman, X. Tan, Y. Zhang, H. Jiang, R. Costa, K.A. Friedrich, R. Kriegel, Advanced Functional Materials, (2021).

[2] Y. Li, W. Zhang, Y. Zheng, J. Chen, B. Yu, Y. Chen, M. Liu, Chem Soc Rev, 46 (2017) 6345-6378.

[3] Y. Ling, X. Wang, Z. Ma, K. Wei, Y. Wu, M. Khan, K. Zheng, S. Shen, S. Wang, Journal of Materials Science, 55 (2019) 1-23.

[4] X. Zhu, W. Yang, Green Chemistry and Sustainable Technology, (2017).

[5] W. Fang, F. Liang, Z. Cao, F. Steinbach, A. Feldhoff, Angew Chem Int Ed Engl, 54 (2015) 4847-4850.

[6] J. Ma, Y. Pan, Y. Wang, Y. Chen, Journal of Power Sources, 509 (2021).

[7] D. Poetzsch, R. Merkle, J. Maier, Advanced Functional Materials, 25 (2015) 1542-1557.

[8] M. Papac, V. Stevanović, A. Zakutayev, R. O'Hayre, Nature Materials, (2020) 1-13.

[9] Z. Gao, L.V. Mogni, E.C. Miller, J.G. Railsback, S.A. Barnett, Energy & Environmental Science, 9 (2016) 1602-1644.

[10] S.P. Jiang, International Journal of Hydrogen Energy, 44 (2019) 7448-7493.

[11] C. Li, J.J. Chew, A. Mahmoud, S. Liu, J. Sunarso, Journal of Membrane Science, 567 (2018) 228-260.

[12] A.P. Tarutin, J.G. Lyagaeva, D.A. Medvedev, L. Bi, A.A. Yaremchenko, Journal of Materials Chemistry A, 9 (2021) 154-195.

[13] S. Wang, T. Kobayashi, M. Dokiya, T. Hashimoto, Journal of the Electrochemical Society, 147 (2000) 3606-3609.

[14] L. Lei, J. Zhang, Z. Yuan, J. Liu, M. Ni, F. Chen, Advanced Functional Materials, (2019) 1903805.

[15] Q. Zhang, Y. Guo, J. Ding, G. Jiang, J. Wen, Journal of Power Sources, 472 (2020).

[16] E.Y. Pikalova, E.G. Kalinina, Russian Chemical Reviews, 90 (2021) 703-749.

[17] G. Li, Y. Gou, R. Ren, C. Xu, J. Qiao, W. Sun, Z. Wang, K. Sun, Journal of Power Sources, 508 (2021).

[18] J.-I. Lee, K.-Y. Park, H. Park, H. Bae, M. Saqib, K. Park, J.-S. Shin, M. Jo, J. Kim, S.-J. Song, E.D. Wachsman, J.-Y. Park, Journal of Power Sources, 510 (2021).

[19] Z. Zhao, J. Cui, M. Zou, S. Mu, H. Huang, Y. Meng, K. He, K.S. Brinkman, J. Tong, Journal of Power Sources, 450 (2020).

[20] W. Li, B. Guan, T. Yang, Z. Li, W. Shi, H. Tian, L. Ma, T.L. Kalapos, X. Liu, Journal of Power Sources, 495 (2021).

[21] Z. Tao, M. Fu, Y. Liu, Y. Gao, H. Tong, W. Hu, L. Lei, L. Bi, International Journal of Hydrogen Energy, 47 (2022) 1947-1953.

[22] X.-Y. Wu, A.F. Ghoniem, Progress in Energy and Combustion Science, 74 (2019) 1-30.

[23] J. Richter, P. Holtappels, T. Graule, T. Nakamura, L.J. Gauckler, Chemical Monthly, 140 (2009) 985-999.

[24] I. Riess, Solid State Ionics, 91 (1996) 221-232.

[25] E. Naumovich, V. Kharton, F. Marques, Measurement of Oxygen Ionic Transport in Mixed Conductors, in: Mixed Ionic Electronic Conducting Perovskites for Advanced Energy Systems, Springer, 2004, pp. 185-198.

[26] J. Patakangas, Y. Ma, Y. Jing, P. Lund, Journal of Power Sources, 263 (2014) 315-331.

[27] J. Zhang, L. Lei, F. Zhao, F. Chen, M. Han, Electrochimica Acta, 340 (2020).

[28] J.H. Kim, J. Hong, D.-K. Lim, S. Ahn, J. Kim, J.K. Kim, D. Oh, S. Jeon, S.-J. Song, W. Jung, Energy & Environmental Science, (2022).

[29] A. Seong, J. Kim, D. Jeong, S. Sengodan, M. Liu, S. Choi, G. Kim, Advanced Science, (2021).

[30] G. Ma, F. Zhang, J. Zhu, G. Meng, Chemistry of materials, 18 (2006) 6006-6011.

[31] F. Zhang, Q. Yang, B. Pan, R. Xu, H. Wang, G. Ma, Materials Letters, 61 (2007) 4144-4148.

[32] D. Han, X. Liu, T.S. Bjørheim, T. Uda, Advanced Energy Materials, (2021).

[33] H. Zhu, S. Ricote, C. Duan, R.P. O'Hayre, R.J. Kee, Journal of The Electrochemical Society, 165 (2018) F845-F853.

[34] H. Zhu, S. Ricote, C. Duan, R.P. O'Hayre, D.S. Tsvetkov, R.J. Kee, Journal of The Electrochemical Society, 165 (2018) F581-F588.

[35] P.-M. Geffroy, A. Pons, E. Béchade, O. Masson, J. Fouletier, Journal of Power Sources, 360 (2017) 70-79.

[36] J. Patterson, Journal of the Electrochemical Society, 118 (1971) 1033.

[37] W. Lai, S.M. Haile, Journal of the American Ceramic Society, 88 (2005) 2979-2997.

[38] D. Han, T. Uda, Journal of Materials Chemistry A, 6 (2018) 18571-18582.

[39] R. Qiu, W. Lian, Y. Ou, Z. Tao, Y. Cui, Z. Tian, C. Wang, Y. Chen, J. Liu, L. Lei, J. Zhang, Journal of Power Sources, 505 (2021).

[40] S. Ricote, H. Zhu, W.G. Coors, C. Chatzichristodoulou, R.J. Kee, Solid State Ionics, 265 (2014) 22-28.

[41] I. Riess, D. Tannhauser, Solid State Ionics, 7 (1982) 307-315.

[42] I. Zvonareva, X.-Z. Fu, D. Medvedev, Z. Shao, Energy & Environmental Science, (2022).

[43] H. Zhu, S. Ricote, W.G. Coors, C. Chatzichristodoulou, R.J. Kee, Solid State Ionics, 268 (2014) 198-207.

[44] M. Søgaard, P. Vang Hendriksen, M. Mogensen, Journal of Solid State Chemistry, 180 (2007) 1489-1503.

[45] M. Yang, E. Bucher, W. Sitte, Journal of Power Sources, 196 (2011) 7313-7317.

[46] C.B. Gopal, S.M. Haile, J. Mater. Chem. A, 2 (2014) 2405-2417.

[47] C.C. Wang, T. Becker, K. Chen, L. Zhao, B. Wei, S.P. Jiang, Electrochimica Acta, 139 (2014) 173-179.

[48] S. Wang, H. Inaba, H. Tagawa, M. Dokiya, T. Hashimoto, Solid State Ionics, 107 (1998) 73-79.

[49] M.V. Patrakeev, I.A. Leonidov, V.L. Kozhevnikov, Journal of Solid State Electrochemistry, 15 (2010) 931-954.

[50] D. Han, K. Toyoura, T. Uda, ACS Applied Energy Materials, 4 (2021) 1666-1676.

[51] M.J. Zayas-Rey, L. dos Santos-Gómez, D. Marrero-López, L. León-Reina, J. Canales-Vázquez, M.A.G. Aranda, E.R. Losilla, Chemistry of Materials, 25 (2013) 448-456.

[52] C. Wagner, Zeitschrift für Elektrochemie, Berichte der Bunsengesellschaft für physikalische Chemie, 60 (1956) 4-7.

[53] S. Wang, L. Wu, J. Gao, Q. He, M. Liu, Journal of Power Sources, 185 (2008) 917-921.

[54] V. Gorelov, Elektrokhimiya, 24 (1988) 1380-1381.

[55] M. Liu, H. Hu, Journal of the Electrochemical Society, 143 (1996) L109-L112.

[56] J.R. Frade, V.V. Kharton, A.A. Yaremchenko, E.V. Tsipis, Journal of Solid State Electrochemistry, 10 (2005) 96-103.

[57] N. Danilov, J. Lyagaeva, G. Vdovin, D. Medvedev, A. Demin, P. Tsiakaras, ACS Applied Materials & Interfaces, 9 (2017) 26874-26884.

[58] M. Liu, J. Winnick, Solid State Ionics, 118 (1999) 11-21.

[59] D. Huan, W. Wang, Y. Xie, N. Shi, Y. Wan, C. Xia, R. Peng, Y. Lu, Journal of Materials Chemistry A, 6 (2018) 18508-18517.

[60] S. Shen, Y. Yang, L. Guo, H. Liu, Journal of Power Sources, 256 (2014) 43-51.

[61] K.L. Duncan, E.D. Wachsman, Journal of the Electrochemical Society, 156 (2009) B1030.

[62] F. Iguchi, N. Sata, H. Yugami, Journal of Materials Chemistry, 20 (2010).

[63] M. Shirpour, R. Merkle, C.T. Lin, J. Maier, Physical chemistry chemical physics : PCCP, 14 (2012) 730-740.

[64] H. Näfe, Electrochimica Acta, 56 (2011) 9004-9010.

[65] D. Han, Y. Noda, T. Onishi, N. Hatada, M. Majima, T. Uda, International Journal of Hydrogen Energy, 41 (2016) 14897-14908.

[66] I. Riess, Solid State Ionics, 44 (1991) 207-214.

[67] M. Liu, Journal of the Electrochemical Society, 144 (1997) 1813-1834.

[68] J.-H. Zhang, L.-B. Lei, D. Liu, F.-Y. Zhao, M. Ni, F. Chen, Journal of Power Sources, 400 (2018) 333-340.

[69] D.P. Sutija, T. Norby, P. Björnbom, Solid State Ionics, 77 (1995) 167-174.

[70] H.K. Bentzer, N. Bonanos, J.W. Phair, Solid State Ionics, 181 (2010) 249-255.

[71] D. Pérez-Coll, G. Heras-Juaristi, D.P. Fagg, G.C. Mather, Journal of Power Sources, 245 (2014) 445-455.

[72] D. Pérez-Coll, G. Heras-Juaristi, D.P. Fagg, G.C. Mather, Journal of Materials Chemistry A, 3 (2015) 11098-11110.

[73] H.I. Yoo, M. Martin, Physical chemistry chemical physics : PCCP, 12 (2010) 14699-14705.

[74] J.-Y. Yoon, J. In Yeon, H.-I. Yoo, Solid State Ionics, 213 (2012) 22-28.

[75] P. Fabry, M. Kleitz, C. Déportes, Journal of Solid State Chemistry, 5 (1972) 1-10.

[76] A. Yaremchenko, V. Kharton, E. Naumovich, V. Samokhval, Solid State Ionics, 111 (1998) 227-236.

[77] V.V. Kharton, A.L. Shaula, N.P. Vyshatko, F.M.B. Marques, Electrochimica Acta, 48 (2003) 1817-1828.

[78] V. Kharton, A. Viskup, F. Figueiredo, E. Naumovich, A. Yaremchenko, F. Marques, Electrochimica acta, 46 (2001) 2879-2889.

[79] V. Kharton, A. Yaremchenko, A. Viskup, G. Mather, E. Naumovich, F. Marques, Solid State Ionics, 128 (2000) 79-90.

[80] A.A. Yaremchenko, V.V. Kharton, E.N. Naumovich, A.A. Tonoyan, V.V. Samokhval, Journal of Solid State Electrochemistry, 2 (1998) 308-314.

[81] M.H. Hebb, The journal of chemical physics, 20 (1952) 185-190.

[82] G.D. Nam, J.-H. Ahn, J.H. Joo, Electrochimica Acta, 260 (2018) 855-860.

[83] L.M. Friedman, K.E. Oberg, W.M. Boorstein, R.A. Rapp, Metallurgical Transactions, 4 (1973) 69-74.

[84] K.-R. Lee, J.-H. Lee, H.-I. Yoo, Solid State Ionics, 181 (2010) 724-729.

[85] C. Chatzichristodoulou, P.V. Hendriksen, Physical chemistry chemical physics : PCCP, 13 (2011) 21558-21572.

[86] S. Lübke, H.-D. Wiemhöfer, Solid State Ionics, 117 (1999) 229-243.

[87] X. Guo, J. Maier, Solid State Ionics, 130 (2000) 267-280.

[88] I. Riess, Solid State Ionics, 51 (1992) 219-229.

[89] I. Riess, Solid state ionics, 66 (1993) 331-336.

[90] T. Shimonosono, Y. Hirata, Y. Ehira, S. Sameshima, T. Horita, H. Yokokawa, Solid State Ionics, 174 (2004) 27-33.

[91] G. Dudley, B. Steele, Journal of Solid State Chemistry, 31 (1980) 233-247.

[92] R. Safadi, I. Riess, Solid state ionics, 58 (1992) 139-154.

[93] X. Li, H. Zhao, F. Gao, Z. Zhu, N. Chen, W. Shen, Solid State Ionics, 179 (2008) 1588-1592.

[94] T. Miruszewski, J. Karczewski, B. Bochentyn, P. Jasinski, M. Gazda, B. Kusz, Journal of Physics and Chemistry of Solids, 91 (2016) 163-169.

[95] L.A. Dunyushkina, V.P. Gorelov, Solid State Ionics, 253 (2013) 169-174.

[96] M.J. Zayas-Rey, L. dos Santos-Gomez, A. Cabeza, D. Marrero-Lopez, E.R. Losilla, Dalton Trans, 43 (2014) 6490-6499.

[97] C. Wagner, Progress in solid state chemistry, 10 (1975) 3-16.

[98] Y. Song, Y. Chen, W. Wang, C. Zhou, Y. Zhong, G. Yang, W. Zhou, M. Liu, Z. Shao, Joule, 3 (2019) 2842-2853.

[99] P.-M. Geffroy, E. Deronzier, J. Gillibert, P. Munch, T. Chartier, J. Fouletier, Journal of The Electrochemical Society, 167 (2020).

[100] H. Bouwmeester, H. Kruidhof, A. Burggraaf, Solid state ionics, 72 (1994) 185-194.

[101] M.C. Steil, J. Fouletier, P.M. Geffroy, Journal of Membrane Science, 541 (2017) 457-464.

[102] J.H. Joo, G.S. Park, C.-Y. Yoo, J.H. Yu, Solid State Ionics, 253 (2013) 64-69.

[103] S.J. Xu, W.J. Thomson, Chemical Engineering Science, 54 (1999) 3839-3850.

[104] T. Norby, Y. Larring, Solid State Ionics, 136 (2000) 139-148.

[105] S. Xie, W. Liu, K. Wu, P. Yang, G. Meng, C. Chen, Solid State Ionics, 118 (1999) 23-28.

[106] I.P. Marozau, D. Marrero-López, A.L. Shaula, V.V. Kharton, E.V. Tsipis, P. Núñez, J.R. Frade, Electrochimica Acta, 49 (2004) 3517-3524.

[107] V. Kharton, A. Viskup, E. Naumovich, N. Lapchuk, Solid State Ionics, 104 (1997) 67-78.

[108] S.Y. Kim, J. Li, Energy Material Advances, 2021 (2021) 1-15.

[109] C. Hwang, J. Lee, J. Jeong, E. Lee, J. Kim, S. Kim, C. Yang, H.-K. Song, Journal of Materials Chemistry A, 9 (2021) 4751-4757.

[110] Y. Chen, Z. Wang, X. Li, X. Yao, C. Wang, Y. Li, W. Xue, D. Yu, S.Y. Kim, F. Yang, A. Kushima, G. Zhang, H. Huang, N. Wu, Y.W. Mai, J.B. Goodenough, J. Li, Nature, 578 (2020) 251-255.

[111] R. Amin, Y.-M. Chiang, Journal of The Electrochemical Society, 163 (2016) A1512-A1517.

[112] S.B. Ma, H.J. Kwon, M. Kim, S.M. Bak, H. Lee, S.N. Ehrlich, J.J. Cho, D. Im, D.H. Seo, Advanced Energy Materials, 10 (2020) 2001767.

Captions:

Figure 1 Scientometric analysis of SCI papers from 2000 to 2021 (a) annual SCI papers about MIEC materials; (b) co-occurrence network of keywords in SCI papers; (c) annual SCI papers about conduction properties of MIEC materials; (d) annual SCI papers about TIEC materials.

Figure 2 Five most widely used methods for determining electrical meconduction properties of MIEC oxides

Figure 3 (a) Schematic of Patterson diagram; (b) schematic of test setup for measuring total conductivity by electrochemical impedance spectroscopy.

Figure 4 (a) Equivalent circuits for EMF method; (b) schematic of test setup. R_i, $R_{p,r}$, R_e and R_{aux} refer to the ionic resistance, real electrode polarization resistance, electronic

Figure 5 (a) Equivalent circuits for the Faradaic efficiency method; (b) schematic of test setup. R_i, $R_{p,r}$, and R_e refer to the ionic resistance, real electrode polarization resistance and electronic resistance in the cell, respectively. I_i, I_e and I_{ext} are ionic current, electronic current and external current, respectively.

Figure 6 Schematic of the Hebb-Wagner method

Figure 7 Schematic view of a thick-film polarization cell in plane geometry [82].

Figure 8 (a) Schematic of gas permeation through mixed oxygen-ionic and electronic conductors; (b) schematic of gas permeation through mixed protonic and electronic conductors; (c) schematic of experimental setup for gas permeation method.